

MOL #50971

# Structural basis of NR2B-selective antagonist recognition by NMDA receptors

**Laetitia Mony, Lucie Krzaczkowski, Manuel Léonetti, Anne Le  
Goff, Karine Alarcon, Jacques Neyton, Hughes-Olivier Bertrand,  
Francine Acher and Pierre Paoletti**

LM, LK, ML, ALG, JN and PP :  
Laboratoire de Neurobiologie, CNRS UMR 8544  
Ecole Normale Supérieure  
46 rue d'Ulm, 75005 Paris, France

LM, LK and FA :  
Laboratoire de Chimie et Biochimie Pharmacologiques et Toxicologiques, CNRS UMR 8601  
Université Paris Descartes  
45 rue des Saints Pères, 75006 Paris, France

ML : Present address: Laboratory of Molecular Neurobiology and Biophysics, Rockefeller University  
and Howard Hughes Medical Institute, 1230 York Avenue, New York, NY 10021, USA.

KA : Laboratoire de Chimie Bioorganique, CNRS UMR 7175  
Faculté de Pharmacie, Université Louis Pasteur de Strasbourg  
74 route du Rhin, 67401 Illkirch, France

HOB : Accelrys  
Parc Club Orsay Université  
20 rue J. Rostand, 91983 Orsay, France

1

---

This work was supported by Ministère de la Recherche (LM) and by INSERM and ANR (PP)

MOL #50971

Running title: The ifenprodil binding-site on NMDA receptors

Corresponding author: Dr. Pierre Paoletti

[paoletti@biologie.ens.fr](mailto:paoletti@biologie.ens.fr)

Laboratoire de Neurobiologie, CNRS UMR 8544

Ecole Normale Supérieure

46 rue d'Ulm, 75005 Paris, France

Pages: 35

Table: 1

Figures: 7

References: 44

Abstract: 250 words

Introduction: 802 words

Discussion: 1343 words

Non-standard abbreviations:

NMDAR: N-methyl-D-aspartate receptor

iGluR: ionotropic glutamate receptor

NTD: N-terminal domain

ABD: agonist-binding domain

DTPA: diethylenetriamine-pentaacetic acid

MOL #50971

## Abstract

N-methyl-D-aspartate receptors (NMDARs) are ionotropic glutamate receptors (iGluRs) endowed with unique pharmacological and functional properties. In particular, their high permeability to calcium ions confers on NMDARs a central role in triggering long term changes in synaptic strength. Under excitotoxic pathological conditions, as occurring during brain trauma, stroke or Parkinson's and Huntington's diseases, calcium influx through NMDAR channels can also lead to neuronal injury. This argues for the use of NMDAR antagonists as potential therapeutic agents. To date, the most promising NMDAR antagonists are ifenprodil and derivatives, compounds that act as non-competitive inhibitors selective for NMDARs containing the NR2B subunit. Recent studies have identified the large N-terminal domain (NTD) of NR2B as the region controlling ifenprodil sensitivity of NMDARs. We present here a detailed characterization of the ifenprodil binding site using both experimental and computational approaches. 3D homology modelling reveals that ifenprodil fits well in a closed cleft conformation of the NRB NTD; however, ifenprodil can adopt either one of two possible binding orientations of opposite direction. By studying the effects of cleft mutations, we show that only the orientation in which the phenyl moiety points deep towards the NTD hinge is functionally relevant. Moreover, based on our model, we identify novel NTD NR2B residues that are crucial for conferring ifenprodil sensitivity and provide functional evidence that these residues directly interact with the ifenprodil molecule. This work provides a general insight into the origin of the subunit-selectivity of NMDAR non-competitive antagonists and offer clues for the discovery of novel NR2B-selective antagonists.

MOL #50971

## Introduction

NMDA receptors (NMDARs) are glutamate-gated ion channels widely expressed in the central nervous system that mediate a component of excitatory synaptic transmission. NMDARs are essential for normal physiological processes such as brain development, synaptic plasticity, learning and memory (Dingledine et al., 1999). NMDARs are also involved in many brain disorders, triggering an intense interest as potential therapeutic targets. They are best known for their role in excitotoxicity, a process during which excessive glutamate release causes overactivation of NMDARs, accumulation of intracellular calcium and, eventually, neuronal death. Excitotoxicity occurs during many acute (brain trauma, stroke) and chronic neurodegenerative disorders (Alzheimer's, Parkinson's, Huntington's diseases). Overactivity of NMDARs is also observed in epilepsy and chronic pain (Kemp and McKernan, 2002). To counteract the deleterious effects of NMDAR overactivation, extensive efforts have been made to discover potent and selective NMDAR antagonists. In the 1980s, the first compounds to be developed were competitive antagonists and high-affinity channel blockers. However, despite good efficiency against neuronal injury, most of these early NMDARs antagonists failed in clinical trials because of unacceptable side effects including hallucinations, drowsiness, memory and motor deficits (Kemp and McKernan, 2002). One likely explanation for the failure of these first-generation NMDAR antagonists is their lack of subunit specificity. By targeting the agonist-binding domain (competitive antagonists) or the ion pore (channel blockers), these compounds do not discriminate between the various NMDAR subtypes and cause generalized inhibition of NMDAR activity.

*In vivo*, NMDARs occur as multiple subtypes most often composed of NR1 and NR2 subunits. They form heterotetrameric complexes made of two NR1 and two NR2 subunits. While NR1 is encoded by a single gene, the NR2 subunit exists as four subtypes encoded by four different genes (NR2A-D), each with a distinctive spatiotemporal pattern of expression. Different subunit composition imparts different biophysical and pharmacological properties (Cull-Candy and Leszkiewicz, 2004; Paoletti and Neyton, 2007). One of the most exciting recent developments in NMDAR pharmacology has been the identification of highly subtype-selective antagonists that act allosterically (in a non-competitive manner). As a matter of fact, these agents are much better tolerated compared to broad-spectrum NMDAR antagonists (Kemp and McKernan, 2002). The most promising subtype selective compounds are ifenprodil and derivatives, a large family of synthetic compounds that selectively inhibit

MOL #50971

NMDARs containing the NR2B subunit (Williams et al., 1993; Mott et al., 1998; Hatton and Paoletti, 2005). Among them, several highly potent molecules show good efficacy as neuroprotectants and/or pain killers in a variety of animal models (Chizh et al., 2001; Chazot et al., 2004; Gogas, 2006). Importantly, in humans, NR2B-selective antagonists do not induce the adverse side effects usually seen with non-selective NMDAR antagonists, even at maximally neuroprotective doses (Chizh et al., 2001; Gogas, 2006). In spite of these encouraging data, NR2B-selective antagonists have not succeeded in clinical trials yet because of poor oral bioavailability and pharmacokinetic profiles (Kemp and McKernan; 2002). Thus, new potent NR2B-selective antagonists are still in great demand.

The ifenprodil binding site on NMDARs has been mapped to the N-terminal domain (NTD) of the NR2B subunit (Gallagher et al., 1996; Perin-Dureau et al., 2002; Malherbe et al., 2003). The NTD, composed of the first ~380 amino-acids, is present in all eukaryotic iGluR subunits and participates in subunit assembly (Mayer, 2006). In NR2A and NR2B subunits, the NTD also forms a modulatory domain binding the  $Zn^{2+}$  ion, which acts as an endogenous allosteric inhibitor of NMDARs (Choi and Lipton, 1999; Low et al., 2000; Paoletti et al., 2000; Rachline et al., 2005; Gielen et al., 2008). NR2A and NR2B NTDs form discrete modules since they are still capable of binding zinc or ifenprodil when produced in isolation from the remainder of the receptor complex (Perin-Dureau et al., 2002; Rachline et al., 2005; Wong et al., 2005). NMDAR NTDs share weak sequence similarity with some bacterial periplasmic binding proteins like LIVBP (leucine/isoleucine/valine-binding protein; Masuko et al., 1999; Paoletti et al., 2000). Their structure has not been determined yet, but they are thought to fold as two lobes separated by a hinge, similarly to LIVBP. Using a mutagenesis approach, Perin-Dureau et al. (2002) suggested that ifenprodil binds in the central interlobe cleft of NR2B NTD and promotes cleft closure through a hinge-bending motion (Venus-flytrap mechanism). However, despite the plentiful production of ifenprodil-derived NR2B-selective antagonists (Chenard and Menniti, 1999; Nikam and Meltzer, 2002), the binding mode of ifenprodil and its derivatives on NR2B NTD remains ill defined. It is unclear which of the NTD residues directly interact with the ligand and what is the structural basis for the subtype-selective pharmacology conferred by the NTDs. Recently, Marinelli et al. (2007) proposed a model of ifenprodil binding into NR2B NTD but, because no experimental validation was performed, it remains a theoretical proposal. In this study, we combine molecular modelling and functional approaches to provide a realistic 3D model of the NR2B NTD-ifenprodil complex.

MOL #50971

## Materials and Methods

**Molecular biology:** The pcDNA3-based expression plasmids for rat NR1-1a (named NR1 herein), rat NR2A and mouse  $\epsilon 2$  (named NR2B herein), the mutagenesis strategy, the sequencing and the RNA synthesis have been described previously (Paoletti et al., 1997, 2000; Rachline et al., 2005)

**Electrophysiology:** Recombinant NMDA receptors were expressed in *Xenopus laevis* oocytes after coinjection of 30 nL of a mixture of cDNAs (at 10 ng/ $\mu$ L; nuclear injection) or cRNAs (at 10-100 ng/ $\mu$ L) coding for wild-type NR1-a and various NR2B subunits (ratio 1:1). Oocytes were prepared, injected, voltage-clamped and superfused as described previously (Paoletti et al., 1997). The standard external solution contained (in mM): 100 NaCl, 0.3 BaCl<sub>2</sub>, 5 HEPES, 2.5 KOH. The pH was adjusted to 7.3 with HCl. NMDA currents were induced by simultaneous application of saturating concentrations of L-glutamate and glycine (100  $\mu$ M each) and recorded at -60 mV. Zinc solutions were obtained by diluting in the agonist solution a 100 mM ZnCl<sub>2</sub> stock-solution prepared in 0.1 N HCl. In these solutions, zinc was not buffered and the control zinc-free solution was made by adding 10  $\mu$ M diethylenetriamine-pentaacetic acid (DTPA) to chelate trace amounts of contaminant zinc (Paoletti et al., 1997). Ifenprodil was prepared as 100  $\mu$ L aliquots (in bidistilled water) at 10 mM and stored at -20 °C. For pH sensitivity experiments, solutions were prepared according to Gielen et al. (2008). When performing pH dose-response curves, at very alkaline pH values, glutamate and glycine concentrations were adjusted to compensate for the loss of protonation of the  $\alpha$ -amino moiety (pK<sub>a</sub> ~ 9.7 for both L-glutamate and glycine). Thus, for pH of 9.3 and 10.3, glutamate and glycine concentrations were increased by 1.4-fold and 5-fold, respectively. All experiments were performed at room temperature.

**Data analysis:** Data were collected and analyzed using pClamp 9.2 (Axon Instruments, Foster City, CA). They were fitted using Sigmaplot 8.0 (SSPS, Chicago, IL). For ifenprodil dose-response curves, experimental points were fitted using the following Hill equation (Eq. 1):  $I_{\text{ifen}}/I_{\text{control}} = 1 - a/(1 + (IC_{50}/[ifen])^{n_H})$ , where  $I_{\text{ifen}}/I_{\text{control}}$  is the mean relative current, [ifen] is the ifenprodil concentration, IC<sub>50</sub> is the concentration of ifenprodil producing 50% of the maximal inhibition, n<sub>H</sub> is the Hill coefficient and a is the maximal inhibition at the saturating ifenprodil concentration. IC<sub>50</sub>, a and n<sub>H</sub> were set as free parameters. Zinc dose-response

MOL #50971

curves were fitted using the following Hill-derived equation (Eq. 2):  $I_{\text{zinc}}/I_{\text{control}} = 1 - a/(1 + \{IC_{50}/([Zn] + b)\}^n_H)$ , where  $b$  is the contaminant zinc concentration and  $[Zn]$  the added zinc concentration. Following Rachline et al. (2005),  $b$  was set to 100 nM. pH dose-response curves were analysed according to Gielen et al. (2008). Error bars represent the standard deviation (SD) of the mean of relative currents.

**Cysteine affinity labelling:** N-{4-[2-(4-Benzyl-piperidin-1-yl)-propionyl]-phenyl}-2-chloroacetamide (Alarcon et al., 2008, referred as molecule **4**) was prepared at 500 mM in anhydrous DMSO. Initial agonist response ( $I_0$ ) was measured in oocytes. Then each oocyte was removed from the recording chamber and incubated in a 100  $\mu$ L Barth solution (in mM: 88 NaCl, 1 KCl, 0.33  $Ca(NO_3)_2$ , 0.41  $CaCl_2$ , 0.82  $MgSO_4$ , 2.4  $NaHCO_3$ , 10 HEPES, pH adjusted to 7.6 with NaOH) containing gentamycin (50  $\mu$ g/ $\mu$ L), glutamate (100  $\mu$ M), 5,7-dichlorokynurenic acid (40  $\mu$ M) and 500  $\mu$ M of the reactive ifenprodil derivative (**4** or **12**). After 30 min incubation at room temperature, oocytes were washed during 1 min in a Barth solution containing gentamycin (50  $\mu$ g/ $\mu$ L). We verified that, on wt NR1/NR2B receptors, 1 minute of wash-out was sufficient for an almost recovery of the initial agonist-induced response after an application of 500  $\mu$ M of molecule **4**. Then agonist response was measured again ( $I_{\text{incub}}$ ). The ratio  $I_{\text{incub}}/I_0$  is reported for each oocyte. Error bars represent the standard error (SE) of the mean ratio  $I_{\text{incub}}/I_0$ .

In preliminary control experiments, we observed that incubation in 500  $\mu$ M molecule **4** induced a decrease of the NMDA response carried by wt NR1/NR2B receptors ( $I_{\text{incub}}/I_0 = 0.35 \pm 0.06$ ;  $n = 6$ ). An endogenous cysteine, C232, is located in the vicinity of the ifenprodil binding-site of NR2B and could possibly react with compound **4**. However, a similar  $I_{\text{incub}}/I_0$  ratio was found for NR1wt/NR2B-C232A receptors, showing that the irreversible inhibition seen on wt receptors is not due to irreversible labelling of this NTD cleft cysteine. This hypothesis was confirmed by incubating oocytes expressing wt NR1/NR2B receptors in 100  $\mu$ M of the non-reactive ifenprodil molecule, which also yielded a strong decrease in the NMDA response ( $I_{\text{incub}}/I_0 = 0.10 \pm 0.04$ ;  $n = 10$ ) (In this latter experiment, because of the slow wash-out of ifenprodil inhibition [Perin-Dureau et al., 2002], oocytes were washed during 10 min after incubation in ifenprodil). In contrast, incubation in 100  $\mu$ M ifenprodil induced very little irreversible inhibition of receptors truncated for the entire NR2B NTD (NR1wt/NR2B- $\Delta$ NTD) ( $I_{\text{incub}}/I_0 = 0.9 \pm 0.1$ ;  $n = 5$ ) or of receptors containing a single strong ifenprodil binding mutation (NR1/NR2B-D101A or NR1/NR2B-V262D receptors, data not shown). Therefore, at high concentrations, ifenprodil and

MOL #50971

derivatives can induce an NTD-dependent irreversible inhibition of NR2B-containing NMDARs, without involving any covalent binding of these molecules. The magnitude of this non-covalent irreversible effect was found to depend on the affinity of the receptor for the ifenprodil derivative (data not shown).

### **Molecular modelling studies:**

#### *Homology modelling of NR2B NTD*

A sequence alignment of rat NR2A and NR2B NTDs with the agonist-binding domain of mGluR1 was generated according to Malherbe et al. (2003) and further refined using predicted (NR2A and NR2B) and known (mGluR1 agonist-binding domain; PDB code 1ewk:A) secondary structures. Secondary structure elements of NR2A and NR2B NTDs were predicted using PROF predictions (<http://www.predictprotein.org>; Rost and Sander, 1993). Homology models for NR2B NTD were generated by the automated comparative modelling tool MODELER 9.0 (DS Modeling 1.7; Accelrys, San Diego, CA) as described previously (Bertrand et al., 2002). Models were generated by using the coordinates of the mGluR1 agonist-binding domain closed form (PDB code 1ewk: A) and based on the sequence alignment described in Figure 1. The structural quality of the models was assessed according to the MODELER probability density functions as well as Profiles-3D analysis (DS Modeling 1.7; Accelrys). Loops were refined using MODELER. The final selected model was used for docking.

#### *Docking of ifenprodil in the model of NR2B NTD*

Ifenprodil was docked using LigandFit (Venkatachalam et al., 2003) (DS Modeling 1.7; Accelrys). In such a process, the protein is kept rigid while the ligands undergo Monte Carlo conformational searching. 20 poses were generated, clustered, and selected according to their binding mode.

#### *Docking refinement of ifenprodil in NR2B NTD*

The obtained protein–ligand complexes were submitted to energy minimization while tethering the C $\alpha$  trace. This was performed using the CHARMM calculation engine (Brooks et al., 1983; DS Modeling version 1.7; Accelrys). CHARMM was also used to perform 1 ns of molecular dynamics at 298 K. Once the system was equilibrated, snapshots were collected, averaged, and submitted again to energy minimization (Bertrand et al., 2002).

#### *Qualitative pharmacophore models generation*

## MOL #50971

Five molecules having the same activity as ifenprodil were selected. The pharmacophore models were generated by using the qualitative common feature pharmacophore HipHop algorithm (Barnum et al., 1996) of Catalyst 4.11.

MOL #50971

## Results

### **Molecular modelling of the N-terminal domain of NR2B and docking of ifenprodil**

We built a 3D model of the NTD of NR2B using the atomic coordinates of the closed agonist-binding domain (ABD) of the metabotropic glutamate receptor mGluR1 as a template (PDB code 1EWK:A; Kunishima et al., 2000). mGluR1 ABD is indeed another LIVBP-like protein which shares slightly more sequence identity with NR2B NTD than LIVBP does (~12% identity for rat NR2B NTD [protein ID Q00960.1] / rat mGluR1 ABD [protein ID P23385.1] vs ~9% for NR2B NTD/LIVBP [PDB code 2liv\_A]). 3D models were generated using the alignment shown in Figure 1. Because the sequence identity between the NR2B NTD and mGluR1 ABD is very low (~12%), we based our alignment according to known (mGluR1 ABD) and predicted (NR2B NTD) secondary structure elements (Figure 1). In the loops putatively lining the central cleft of NR2B NTD (Perin-Dureau et al., 2002; Rachline et al., 2005), we also imposed that residues previously shown to control zinc and/or ifenprodil inhibition should be aligned with residues pointing towards the glutamate binding cleft of mGluR1 ABD. This is obviously a strong constraint. Consequently, we took special care in our subsequent functional experiments to assay the role of these residues pointing towards the NR2B NTD cleft.

The structural quality of the generated 3D models was assessed according to the MODELER probability density functions (PDF energy), as well as Profiles-3D analysis (P3D score). The structural quality of the models was further improved by individually refining loops lining the binding cleft. The final NR2B NTD model showed a P3D score of 151.66 over 166.35 (91% of the maximal expected score) and exhibited no misfolded region around the binding cleft, attesting the overall goodness of the chosen model. We also verified that, in addition to its high score, this model showed a good concordance to the imposed constraint (residues controlling zinc and/or ifenprodil sensitivity pointing towards the interlobe cleft of the NTD). This was indeed the case (see Figure 2). It remains however, that, because the sequences of the NR2B NTD and mGluR1 ABD share such a low sequence identity, the orientations of residues side-chains are rather imprecise. Thorough functional validation of this model is therefore mandatory to attest its biological relevance.

MOL #50971

We then docked ifenprodil in erythro configuration, the synthesis of ifenprodil being diastereoselective (Avenet et al., 1996), into the interlobe cleft of the modelled NR2B NTD, using LigandFit (see Methods). Docking experiments did not reveal a unique binding mode for ifenprodil. Rather, we found that ifenprodil could bind to the NTD of NR2B with two opposite orientations: either with its phenol group close to the entrance of the cleft and its benzyl group contacting the interlobe hinge (orientation 1), or vice-versa (orientation 2). Each orientation was further refined by 1 ns of molecular dynamics (see Methods), to yield the two models shown in Figure 2 (Figure 2A with orientation 1 and Figure 2B with orientation 2). In both models, ifenprodil binds in extended conformations that correspond to low energy conformations in the solvent. Moreover, the ifenprodil molecule makes interactions with both lobes.

We next sought to verify that the conformations of ifenprodil found after molecular dynamics in both orientations were likely to be bioactive conformations. Indeed, ifenprodil is a flexible molecule and the conformation with which it actually binds to the NTD is unclear. The bioactive conformation of a ligand can be predicted by the use of qualitative common feature pharmacophore models (Barnum et al., 1996). A common feature pharmacophore model describes the 3D arrangement of the shared electronic properties required for the activity of a set of molecules on their receptor. To build the pharmacophore model of ifenprodil-like molecules, we used a dataset of five molecules having similar activities to ifenprodil on wt NR1/NR2B receptors (see supplementary Table S1). To obtain a relevant pharmacophore model, we chose rigid molecules with distinct chemical structures. The presence of molecules more rigid than ifenprodil, like those containing an acetylenic linker (second and third molecules of Table S1), is important to limit the number of 3D arrangements of the different pharmacophore features. From this dataset, several pharmacophore models were generated and we selected the pharmacophore with the highest rank. We obtained a four-point pharmacophore composed of two aromatic, one positive ionisable and one H-bond donor features (Figure 3A). The pharmacophore model obtained is consistent with the previously published structure-activity relationship (SAR) data (Tamiz *et al.*, 1998; Chenard and Menniti, 1999 and see below) and predicts an extended conformation of ifenprodil. The two conformations of ifenprodil found after molecular dynamics (orientations 1 and 2) were then mapped to the pharmacophore model. As shown in figure 3B and C, both conformations closely matched the pharmacophore. The conformations of ifenprodil found in the docking models are therefore likely to be both bioactive

MOL #50971

conformations. Which of the two orientations of ifenprodil is the actual bioactive one, remains to be elucidated.

### **Ifenprodil interactions in its binding pocket**

Investigations of the structure-activity relationships (SAR) of ifenprodil derivatives have established that there are common important structural features for this family of compounds (Tamiz *et al.*, 1998; Chenard and Menniti, 1999). There are four features: (i) a phenyl moiety (ring A) interacting with a hydrophobic pocket; (ii) a positively charged central nitrogen atom, which can make ionic or charge-dipole interactions with a H-bond acceptor; (iii) a second phenyl group (ring B) coupled with a H-bond donor that can make both hydrophobic and polar interactions; (iv) a distance separating ring A from ring B of 10-12 Å (linker region). Importantly, the two models described above obey these structural requirements. Moreover, they are overall consistent with the previously published mutagenesis data (Perin-Dureau *et al.*, 2002). Indeed, two out of the four residues found to have a strong effect on ifenprodil sensitivity following mutagenesis (I150, F176; IC<sub>50</sub> more than 60-fold higher than for wild-type [wt] NR2B-containing receptors) are found to be in direct atomic contact with the ifenprodil molecule, irrespective of the orientation 1 or orientation 2 model (Figure 2). The third residue, D101, is also directly interacting with ifenprodil in model 1 but not in model 2 where it is further apart from the ligand. Finally, the fourth residue, F182, is buried in lobe II and cannot contact ifenprodil (Figure 2). However, this residue has been shown to control sensitivity of NR1/NR2B receptors to both ifenprodil and zinc (Rachline *et al.*, 2005), two NR2B NTD ligands of very different chemical nature, indicating that it might be involved in the global structuring of the NTD. Moreover, F182 interacts with Y231, a residue that directly interacts with ifenprodil (see below). Thus, in addition to its global structural role, F182 may also control ifenprodil binding in an indirect manner, via the correct positioning of Y231.

In both orientations, ifenprodil shares common hydrophobic interactions with the receptor. Thus, the aromatic ring close to the hinge of the NR2B NTD is in a hydrophobic pocket mostly composed of isoleucine 150, tyrosine 231, leucine 261 and valine 262 side chains (Figure 2). The direct interaction between I150 and ifenprodil fits well with the finding that mutation of I150 into a shorter alanine strongly and selectively affects ifenprodil inhibition (inhibition by zinc, the other NR2B NTD ligand is not affected; Rachline *et al.*,

MOL #50971

2005). A similar situation applies for L261, a residue which interacts with ifenprodil through its side chain C $\beta$ . In contrast, mutation V262A was shown to have only a modest effect on ifenprodil sensitivity (Perin-Dureau et al., 2002), a result which, at first sight, seems difficult to reconcile with our observation that V262 directly contacts ifenprodil in the models. However, the absence of effect of the valine to alanine mutation could be due to the fact that this mutation does not change the polarity of the residue, and therefore has little impact on ifenprodil binding. Obviously, additional substitutions of valine 262 need to be tested to validate this interaction (see below).

Tyrosine 231 is another residue contacting the ifenprodil aromatic group in the hinge region. In fact, in both orientation 1 and orientation 2 models, Y231 appears to be engaged in multiple interactions not only with the ligand but also with other residues controlling ifenprodil sensitivity such as L261, I150 and F182 (through  $\pi$ -stacking or Van der Waals interactions). The effects of mutations at NR2B-Y231 on ifenprodil sensitivity have not been reported so far. From our models, we expect substitutions at this position to significantly affect ifenprodil inhibition (see below).

At the entrance of the cleft, the aromatic ring of the ifenprodil molecule, in both models, is contacting valine 42, which was also found to exert some control of ifenprodil inhibition (Perin-Dureau et al., 2002). Moreover, the aliphatic chain linking the two aromatic moieties is making Van der Waals contacts with phenylalanine 176 and the carbon chain of lysine 234, two residues that also selectively control ifenprodil inhibition (Rachline et al., 2005). Interestingly, K234 makes an ionic interaction with aspartates 265 and 267 (lobe II), and glutamate 47 (lobe I); accordingly, it may neutralise the electrostatic repulsion between these three residues when the domain closes.

The main differences between the two models stand in the polar interactions. While the central positively-charged amino group of ifenprodil, in orientation 1, makes a coulombian interaction with aspartate 101, in orientation 2, it interacts with another aspartate (D104). In these models, D101 and D104 also make a charge-dipole interaction with the linker's hydroxyl group. Mutation of D101 into an alanine has been shown to strongly affect ifenprodil sensitivity (Rachline et al., 2005). Model 1 accounts well for this result. However, D101 has also a very marked effect on zinc sensitivity (Rachline et al., 2005). This suggests that D101 may either be a common key residue for the coordination of both ifenprodil and zinc, or, alternatively, that it may play a more global structural role in the NR2B NTD. On the other hand, the mutation of D104 into an alanine has a relatively important effect on ifenprodil inhibition ( $IC_{50}$  22-fold higher than for wt) and no effect on zinc inhibition, making

MOL #50971

it a potential candidate to directly bind ifenprodil (Rachline et al., 2005). This latter result is consistent with the orientation 2 model, in which D104 interacts with the amino group and the linker's hydroxyl group. Orientation 1, in contrast, cannot account for the selective effect of D104, as this residue is not pointing towards ifenprodil in the corresponding model. It is important to note, however, that the region containing these two aspartates (loop  $\beta 3-\alpha 3$ ) is very different from the corresponding loop of mGluR1, so that its modelled structure is rather uncertain. Hence, at this stage, there is still a doubt concerning which residue is interacting with the amino group.

Ifenprodil phenolic group (B ring with H-bond donor) interacts with completely different residues depending on its orientation in the NR2B NTD central cleft. In orientation 1 model, ifenprodil phenolic group makes hydrogen bonds with residues located at the entrance of the cleft: T76 and D77 from lobe I, and D206 from lobe II, thus facilitating the closure of the NTD. On the contrary, ifenprodil phenolic group with orientation 2 makes hydrogen bonds with residues from the hinge, deep in the cleft: Q153 and Y282. None of these polar residues (T76, D77, D206, Q153 and Y282) have been mutated yet. Knowing the effect of their mutation is expected to help discriminate between the two models (see below).

Overall, the two proposed models appear to fit satisfactorily with the previously published mutagenesis data (Perin-Dureau et al., 2002; Rachline et al., 2005), although a doubt remains concerning the residues interacting with the amino group of ifenprodil. The good concordance between the molecular modelling results and the previously published functional data is a first assessment of the validity of the proposed models. However, the role of a few residues is still difficult to interpret, such as E106 and E236. These residues have been shown previously to selectively control ifenprodil inhibition, but they do not contact ifenprodil in both of our models. E106 is far from ifenprodil, pointing outside the cleft. E236 is buried in lobe II, but its carboxylic group is making hydrogen bonds with T233 hydroxyl group, thus making the methyl group of T233 point towards ifenprodil (Figure 2). E236 could therefore act indirectly, via T233, this latter residue participating in the control of ifenprodil inhibition (Perin-Dureau et al, 2002). To discriminate between the two orientations of ifenprodil and further attest the relevance of the chosen model, we used the two complementary functional validation methods developed below.

MOL #50971

## **D206, Y231 and V262: three new key residues controlling ifenprodil inhibition**

The two models of ifenprodil binding highlighted seven residues that could directly interact with ifenprodil (D206, T76, D77, Q153, Y231, V262 and Y282), but that had not been mutated yet (except for V262, which had only been mutated into alanine, a rather conservative substitution). If these models are valid, the mutation of these residues with appropriate substitutions should substantially affect ifenprodil inhibition.

The mutation of V262 into an alanine modestly affects ifenprodil sensitivity of wt NR1/NR2B receptors (Perin-Dureau et al., 2002). As previously mentioned, the absence of effect could be due to the fact that alanine is still able to make a hydrophobic interaction with the ifenprodil molecule. To verify this hypothesis, we made multiple substitutions of V262 into either hydrophobic residues of different sizes (glycine, isoleucine and phenylalanine) or into a weakly polar (cysteine) or a charged (glutamate) residue. Typical current traces for three different mutated and wt NR1/NR2B receptors are shown in Figure 4A. Whereas substitution of V262 into an isoleucine slightly increases inhibition by 300 nM ifenprodil ( $75 \pm 7\%$  [n = 5] vs  $63 \pm 6\%$  inhibition for wt [n = 9]), mutations V262F or V262D almost completely abolish inhibition by 300 nM ifenprodil ( $9 \pm 3\%$  inhibition each [n = 3-4]). Ifenprodil full dose-response curves confirm that mutation of V262 into a bulky phenylalanine or a charged acidic aspartate strongly decreases ifenprodil sensitivity (50-fold rightward shift in  $IC_{50}$ ) while mutation into an isoleucine has an opposite effect, slightly increasing ifenprodil sensitivity (1.8-fold leftward shift in  $IC_{50}$ ; Figure 4B and Table 1). The very low ifenprodil sensitivity of NR1/NR2B-V262F is likely to be due to the bulkiness of the phenylalanine residue, thus hindering ifenprodil binding to lobe II. Similarly, in NR1/NR2B-V262D receptors, the presence of an aspartate in a hydrophobic pocket is expected to strongly disrupt ifenprodil binding to lobe II by electrostatic repulsion with the negative partial charges of the aromatic ring. In contrast, adding a supplemental methyl group, as occurring with the isoleucine mutation, may increase ifenprodil sensitivity by reinforcing hydrophobic interactions between the NTD and its ligand. We also found that mutation of V262 into a small weakly polar residue (cysteine) induces only a modest shift in ifenprodil sensitivity (2-fold rightward shift in  $IC_{50}$ ; Table 1), comparable to the shift observed with the alanine substitution. Finally, mutation of V262 into a glycine, which removes any possible side chain interaction with ifenprodil, has a significantly larger effect on ifenprodil sensitivity, increasing ifenprodil  $IC_{50}$  6 fold (Figure 4B). Contrasting with these side-chain specific effects of V262

MOL #50971

mutations on ifenprodil sensitivity, zinc sensitivity was not, or only weakly, affected by any of the V262 mutations. In particular, mutations NR2B-V262F and NR2B-V262D that yield the strongest impairments of ifenprodil inhibition had only little effect on zinc sensitivity (Figure 4 and Table 1). The differential and selective effects of the various V262 mutations of ifenprodil sensitivity strongly support a model in which V262 makes a direct hydrophobic interaction with ifenprodil.

Tyrosine 231 is an additional residue potentially key for ifenprodil binding. In both orientation 1 and orientation 2 models, Y231 directly interacts through its aromatic ring with ifenprodil ring A (orientation 1) or B (orientation 2). The aromatic ring of Y231 also makes direct contact with the side chains of F182, L261 and I150, these two latter residues being also in direct interaction with ifenprodil. It thus appears that Y231 is at the center of a large hydrophobic cluster that forms part of the hydrophobic pocket where ifenprodil ring A (or B) nestles. Accordingly, mutations of Y231 are expected to significantly alter ifenprodil sensitivity. This is precisely what we observed. Replacing Y231 by a cysteine or an alanine to disrupt the interactions described above resulted in a very strong shift in ifenprodil sensitivity (~200- and ~600-fold shift in  $IC_{50}$ , respectively; Figure 5 and Table 1). These effects are larger than for any other single point mutant studied so far. In fact, the sensitivity of NR1/NR2B-Y231A receptors to ifenprodil is very close to the one of NR1/NR2B- $\Delta$ NTD receptors (receptors deleted for the entire NR2B NTD), demonstrating that substituting Y231 by an alanine completely disrupts the ifenprodil binding site. In contrast, zinc sensitivity is only weakly affected by the A (or C) mutation (~2-fold shift in  $IC_{50}$ ; Figure 5), excluding the possibility that Y231 mutations exert their effects through an indirect global structure disruption.

We also assessed the proton sensitivity of receptors containing mutations at V262 and Y231. Indeed, protons are potent inhibitors of NR1/NR2B receptors ( $H^+$   $IC_{50}$  of pH ~7.3 close to the physiological pH) and ifenprodil has been proposed to inhibit receptor activity through an enhancement of tonic proton inhibition (Mott et al., 1998). It could therefore be that the reduced ifenprodil inhibition that we observed on the mutant receptors reflects a decrease in pH sensitivity. To verify if such is the case, we determined the pH sensitivity of the mutant receptors that yield the strongest decrease in ifenprodil sensitivity, i.e. NR1/NR2B-V262F and NR1/NR2B-Y231A ( $\geq 50$ -fold shift in ifenprodil  $IC_{50}$ ; Table 1). We also determined pH sensitivity of receptors containing either the NR2B-D101A or the NR1/NR2B-F176A, two mutations that we previously showed to strongly affect ifenprodil sensitivity (Perin-Dureau et al., 2002). As shown in Figure S1, none of these mutations have a significant effect on pH

MOL #50971

sensitivity (pH IC<sub>50</sub> of 7.52 [n = 4], 7.46 [n = 4], 7.50 [n = 4] and 7.39 [n = 3] for NR1/NR2B-D101A, NR1/NR2B-F176A, NR1/NR2B-Y231A and NR1/NR2B-V262F receptors, respectively, vs 7.45 [n = 4] for wt NR1/NR2B receptors). These data demonstrate that the mutations do not alter ifenprodil sensitivity secondary to changes in pH sensitivity. Rather, they provide further validation that the identified residues are likely to be true binding residues and do not act through indirect gating effects.

Because in the two proposed models, both V262 and Y231 make hydrophobic interactions with the aromatic rings of ifenprodil (ring A in orientation 1 or ring B in orientation 2), the above results are of little help to discriminate between orientation 1 and 2. The situation is strikingly different concerning the interactions of the hydroxyl group of ring B. In orientation 2, the ifenprodil phenol moiety is proposed to make hydrogen bonds with two residues from the hinge, glutamine Q153 and tyrosine Y282. The mutation of Q153 into an alanine or a cysteine, to prevent formation of these hydrogen bonds, results only in a very mild shift in ifenprodil sensitivity (1.5 to 2-fold shift in IC<sub>50</sub>; Table 1 and Figure S2A). Similarly, the mutation of Y282 into a cysteine, a serine or a tryptophan induces a modest, whilst stronger, decrease in ifenprodil sensitivity (~4-fold shift in IC<sub>50</sub>; Figure S2C). As the presence of a H-bond donor at the para position of ring B is critical for ifenprodil-like compounds activity (Chenard and Menniti, 1999), and as in orientation 2, ifenprodil phenolic group is in a rather hydrophobic environment, the mutations of either Q153 or Y282 would, in orientation 2, be expected to induce relatively strong effects on ifenprodil sensitivity. This is clearly not what we observed, indicating that the model of ifenprodil binding in orientation 2 is likely not to be correct. Interestingly, the mutations of residues Q153 or Y282 induce a decrease in the maximal level of inhibition produced by ifenprodil (Figures S2A and C). The larger effect is obtained with the Y282S mutation, which yields a maximal inhibition of 66 % (vs 95% on wt NR1/NR2B receptors; Figure S2C). However, because zinc inhibition is not affected by these hinge mutations (Figures S2B and D), it is likely that these latter do not modify the intrinsic gating properties of the receptor, but rather the binding of ifenprodil *per se*. The mechanism underlying the partial nature of NR1/NR2B receptor inhibition by ifenprodil-like compounds is still unknown, but it is conceivable that, in these modified NR2B NTDs, ifenprodil adopts a slightly different position resulting in a decreased level of inhibition of the receptors.

In order to test the validity of the ifenprodil binding model with orientation 1, the three residues that make hydrogen bonds with the phenol moiety in this orientation, T76, D77 and D206, were mutated. To verify that D206 actually acts as a H-bond acceptor, its polarity was

MOL #50971

either conserved (glutamate mutation) or changed by introducing hydrophobic (alanine and phenylalanine), neutral polar (cysteine) or positively charged (lysine) residues. Figures 6A and B show that such mutations of D206 affect both ifenprodil and zinc sensitivity but, depending on the substitution, the amplitude of the effects differs significantly between the two ligands. For zinc sensitivity, we observed a strong correlation with the side chain charge. Firstly, mutating the aspartate into a glutamate (charge conservation) has no effect on zinc sensitivity ( $IC_{50}$  of 0.67  $\mu$ M for NR2B-D206E [ $n = 3$ ] vs 0.70  $\mu$ M for wt receptors [ $n = 15$ ]; Figure 6B). Secondly, the mutant receptors become progressively less sensitive to zinc as the charge of the substituting amino acid becomes more positive (E  $\rightarrow$  C, A, F  $\rightarrow$  K; Figure 6B and Table 1). Interestingly, the mutations of the homologous NR2A residue, D207, had the same phenotype on high-affinity zinc sensitivity of NR1/NR2A receptors (Paoletti et al., 2000). NR2A-D207, located at the entrance of the NTD cleft, was then proposed to provide a favourable electrostatic environment for zinc to access the cleft. Therefore, we propose that, concerning zinc sensitivity, D206 in NR2B may have a similar attractive role. In contrast to the effects seen on zinc sensitivity, we observed that ifenprodil sensitivity is greatly reduced by mutations at D206, whatever the nature of the mutation (Figure 6A). In particular, substitution of D206 by a glutamate, a residue which is still capable of forming H-bonds, but which is one carbon longer, induces a 10-fold decrease in ifenprodil sensitivity (Table 1). Mutation of D206 into a weakly polar (cysteine) or hydrophobic residue (alanine, phenylalanine) produces a much larger decrease in ifenprodil sensitivity (30 to 45-fold shift in  $IC_{50}$ ; Table 1 and Figure 6A). The largest effect is obtained by the mutation of D206 into a lysine (80-fold shift in  $IC_{50}$ ), a bulky and positively charged residue. These results strongly suggest that, in addition to its attractive electrostatic role, D206 is also likely to directly contact the ifenprodil molecule through polar bonds. This result clearly favours orientation 1 model, in which D206 makes a charge-dipole interaction with ifenprodil B-ring hydroxyl group.

The mutation of D77 into a cysteine selectively reduces ifenprodil sensitivity ( $IC_{50}$  18-fold higher than for wt receptors), with no change in zinc sensitivity (Figure S3 and Table 1). Besides, the mutation of T76 into an alanine or a cysteine has a similar phenotype (15-fold shift in ifenprodil  $IC_{50}$ ; very little change in zinc  $IC_{50}$ ; Figures 6C and D and Table 1). These results suggest that T76 and D77 are likely to interact with ifenprodil. Moreover, mutating T76 into a serine, a residue with a conserved alcohol function, but without the methyl group of threonine, only slightly affects ifenprodil sensitivity (<3-fold shift in ifenprodil  $IC_{50}$ ; Figure 6C and Table 1), indicating that the alcohol function of the threonine is an important

MOL #50971

determinant of ifenprodil sensitivity. Thus, T76, through its hydroxyl moiety, is likely to make a hydrogen bond with ifenprodil. Altogether these results show that D206, T76 and D77 control ifenprodil inhibition, whereas Q153 and Y282 do not. These results are fully consistent with ifenprodil binding in the NTD of NR2B in orientation 1.

### **Orienting ifenprodil in its binding-pocket using the cysteine affinity labelling approach**

If site-directed mutagenesis experiments can provide reliable information regarding which residues control sensitivity to a ligand, they are less powerful to discriminate between residues actually directly binding the ligand from residues having more distant structural effects. In our case, the presence of a second ligand of very different chemical nature, the zinc ion, which also binds into NR2B NTD (Rachline et al., 2005), enables to distinguish residues selectively controlling ifenprodil inhibition (considered as truly “binding” residues) from residues controlling both ifenprodil and zinc inhibition (considered as potential “structural” residues). However, for ifenprodil-selective residues, an uncertainty remains whether they are directly in contact with ifenprodil, or whether they belong to its second coordination sphere. Furthermore, site-directed mutagenesis experiments give no direct information about the precise part of the ligand interacting with the highlighted residue. To probe for direct interactions between a precise region of the NTD and a specific part of the ifenprodil molecule, and thus help orientate unequivocally this compound into its binding pocket, we used the cysteine affinity labelling approach (Foucaud et al., 2001). This technique involves the formation of a covalent bond between a cysteine-reactive ligand derivative and a cysteine-substituted receptor, provided that the ligand reactive group and the cysteine are in close proximity (Figure 7A; Foucaud et al., 2001). This strategy was previously applied to explore the glycine-binding site of the NMDAR NR1 subunit (Foucaud et al., 2003), and the results were remarkably consistent with the crystal structure of the NR1 agonist-binding domain (Furukawa and Gouaux, 2003). In our case, we used the reactive ifenprodil derivatives previously developed by Alarcon et al. (2008) and particularly molecule **4**, in which the phenolic hydroxyl group was replaced by a cysteine-reactive chloroacetamide group (Figure 7). Molecule **4** displays the required reactivity towards cysteine, good stability in solution and significant NR2B NTD-mediated antagonist properties at wt NR1/NR2B receptors (IC<sub>50</sub> of 14 μM; Alarcon et al., 2008). Furthermore, the two point mutations NR2B-

MOL #50971

D101A and V262D, that strongly decrease ifenprodil sensitivity (see Table 1), also markedly reduced sensitivity of NR1/NR2B receptors for molecule **4** (inhibition by 10, 30 and 100  $\mu$ M of  $8 \pm 2$  %,  $15 \pm 7$  % and  $20 \pm 3$  %, respectively, for NR1wt/NR2B-D101A receptors [ $n = 3$ ], of  $12 \pm 8$  %,  $17 \pm 5$  % and  $28 \pm 9$  %, respectively, for NR1wt/NR2B-V262D receptors [ $n = 3$ ] vs  $41 \pm 14$  %,  $56 \pm 11$  %,  $81 \pm 6$  %, respectively, for wt NR1/NR2B receptors [ $n = 5$ ]), indicating that molecule **4** is likely to share the same anchoring points as ifenprodil in the NR2B NTD cleft.

To test which of the orientations (orientation 1 or 2) is used by molecule **4**, we substituted residues T76, L205, D206, Q153 and V262 of the NR2B NTD by cysteines. We selected these residues because there are predicted to contact (or be in close vicinity [L205]) the reactive antagonist in the different docking orientations (Figure 2). The initial NMDA current ( $I_0$ ) was measured on oocytes expressing NMDARs containing one of the above cysteine mutations. Oocytes were then incubated in a solution containing a high concentration of molecule **4** (500  $\mu$ M, close to saturation), and after 30 min of incubation, they were washed to remove any reversible binding of compound **4**. After washing, the NMDA current was measured again ( $I_{\text{incub}}$ ). We expected the ratio  $I_{\text{incub}}/I_0$  to be inferior to 1 if compound **4** induced an irreversible labelling of the cysteine-modified receptors, and to be close to 1 if no irreversible labelling occurred. Unexpectedly, however, we found in preliminary control experiments that long incubation times with reagent **4**, but even with the non-reactive ifenprodil molecule, could produce a long-lasting inhibition of wt NR1/NR2B receptors, an effect that is mediated by the binding of the ligand to the NR2B NTD (see Methods). To circumvent this undesired “side” effect, we systematically compared the effects of the reactive ligand on cysteine-substituted NMDARs with those on NMDARs substituted with an alanine at the same position. As an additional control, we checked that, at the positions tested, receptors had similar ifenprodil  $IC_{50}$  values, whether they were mutated into an alanine or a cysteine. This was indeed the case (Table 1). With these precautions in hand, a significant difference between the  $I_{\text{incub}}/I_0$  ratios of alanine and cysteine-substituted receptors is expected to account for an irreversible labelling of the targeted position. As shown in Figure 7B, at positions lining the entrance of the NR2B NTD cleft, i.e. L205 and D206 from lobe II and T76 from lobe I, a significant difference is observed between the  $I_{\text{incub}}/I_0$  ratio of the alanine and the cysteine mutant. This result suggests that compound **4** could specifically react with the NTD at these positions. On the contrary, no significant difference is observed at positions Q153 and V262, close to the hinge. These results are strongly in favour of the orientation 1 docking model in which ifenprodil phenol group is in close vicinity to the entrance of the

MOL #50971

binding cleft, while its phenyl group points in the opposite direction towards the hinge. These results also provide further support towards a direct interaction of the residues T76 and D206 with the phenolic hydroxyl group of ifenprodil, as proposed in the orientation 1 model.

MOL #50971

## Discussion

In the present work, we delineate the structural determinants that are responsible for the high affinity binding of ifenprodil on the NR2B subunit. For that purpose, we have built 3D homology models of ifenprodil docked in its binding pocket and have subjected these models to an extensive experimental validation process based on site-directed mutagenesis and cysteine affinity labelling. A number of important features emerge from this study: first, as evidenced by the stable docking, ifenprodil fits well into the central crevice of the NR2B N-terminal domain modelled according to a closed conformation of the structurally related bilobate agonist-binding domain of mGluR1; second, despite being a rather symmetrical molecule, ifenprodil likely adopts a unique and well-defined orientation within this crevice. Third, ifenprodil appears to interact with residues of both NTD lobes strongly suggesting that it stabilizes a closed cleft conformation of NR2B NTD, much like activating ligands at other LIVBP-like Venus-flytrap domains (Kunishima et al., 2000; Magnusson et al., 2004; Acher and Bertrand, 2005). Fourth, high-affinity ifenprodil binding is achieved through multiple ligand-protein interactions, involving electrostatic and hydrogen bonds together with Van der Waals contacts distributed all along the ifenprodil molecule.

Based on our models, we have identified, in site-directed mutagenesis experiments, five new NR2B NTD residues that are key for high-affinity ifenprodil inhibition of NR1/NR2B receptors: T76, D77, D206, Y231 and V262. Moreover, by performing multiple side-chain substitutions at these positions and by systematically controlling for specificity towards ifenprodil versus zinc, the other known NR2B NTD ligand (Rachline et al., 2005), we obtained strong support for direct interaction between these residues and ifenprodil. This conclusion was strengthened further in the case of NR2B residues D101, F176, Y231 and V262 by showing that mutations at these positions that strongly affect ifenprodil sensitivity (up to >300-fold shift in ifenprodil IC<sub>50</sub> the case of the NR2B-Y231A mutation) do not alter pH sensitivity. Altogether, these mutagenesis results provide a clear experimental validation of our proposed models. They also allowed us to propose an orientation of the ifenprodil molecule in its binding pocket, something that the modelling alone could not achieve. Ifenprodil binds in an extended conformation, almost perpendicular to the plane of the NTD hinge with its phenyl group (ring A) located close to the NTD hinge and its phenol moiety (ring B) pointing towards the entrance of the cleft. We obtained an additional confirmation that this orientation is likely to be functionally relevant by performing cysteine affinity labelling experiments. Indeed, experiments using compound **4**, a thio-reactive ifenprodil

MOL #50971

analogue functionalised at the level of the phenol hydroxyl group, revealed that this compound can react with cysteines introduced at the entrance of the NTD cleft but not with cysteines deep in the cleft near the hinge. Moreover, the fact that compound **4** labels residues from both lobes of the NTD (T76 from lobe I and L205 and D206 from lobe II) strongly supports a model in which binding of ifenprodil promotes closure of NR2B NTD.

However, if mutagenesis experiments gave effects on ifenprodil inhibition easily interpretable, cysteine affinity labelling experiments were harder to settle. First, although applied at a concentration close to saturation, molecule **4** induced only a partial irreversible labelling of the cysteine-mutated receptors as judged by the changes in current amplitude (specific inhibition from 18 % for the L205C mutation to 38 % for the T76C mutation; Figure 7). The partial nature of the irreversible labelling may be due to the low reactivity of compound **4** with free cysteines in solution ( $t_{1/2} = 114$  min in an excess of N-acetylcysteine methyl-ester; Alarcon et al., 2008), although compound **4** is expected to react much faster once bound in NR2B NTD because of presumably close proximity of the thiol reactive group with the introduced cysteines. We also attempted affinity labelling experiments with another cysteine-reactive ifenprodil analogue: compound **12** from Alarcon et al. (2008), containing an isothiocyanate group at the para position in ring A. If ifenprodil does actually bind in NR2B NTD with orientation 1, compound **12** was expected to specifically label cysteines introduced at positions close to the hinge. However, disappointingly, we could not find any position in NR2B NTD where irreversible labelling with this molecule could be observed, neither at positions close to the hinge, nor at positions close to the entrance of the cleft. Assuming our model is valid, this lack of effect could be due to strong structural constraints: from one side, the low intrinsic rotational mobility of the isothiocyanate group, and from the other, the narrowness of the binding pocket near the NTD hinge. These two effects combined may sharply decrease the probability to find a position at which a cysteine could be properly orientated to react with molecule **12** isothiocyanate group.

A model of ifenprodil binding in NR2B NTD, with no experimental validation, was already proposed by Marinelli et al. in 2007. Our model shares only few similarities with theirs, in which ifenprodil has an almost perpendicular orientation. This difference of docking orientation could be explained by the use of a different sequence alignment, especially for some loops located in the binding cleft. which could give rise to a different shape of ifenprodil binding-site. Marinelli et al. propose, like us, an interaction of D101 with both the central positive amino group and the linker's hydroxyl group. They also highlight V262 as a residue in close vicinity to the ifenprodil molecule. However, in their case, V262 interacts with the

MOL #50971

phenol moiety (ring B) while in ours it interacts with the other aromatic ring, the phenyl moiety. There are multiple points in the model of Marinelli et al. (2007) that are difficult to reconcile with experimental results obtained in this and previous studies. For instance, their model does not explain the critical roles of I150 and the newly found Y231 residue, two residues that produce the largest observed shifts in ifenprodil sensitivity when mutated into alanine with no or little effect on zinc sensitivity (Perin-Dureau et al., 2002 and this study). Furthermore, ifenprodil phenol hydroxyl group is proposed to be in close proximity with D265. An alanine mutation of this residue, located in a rather apolar environment, should have therefore a substantial effect on ifenprodil sensitivity. However, such mutation has no effect on ifenprodil sensitivity (Perin-Dureau et al., 2002). Obviously, these data do not substantiate the model obtained by Marinelli et al. (2007).

An interesting and striking observation is that almost all the residues that in our model line the ifenprodil binding pocket by directly interacting with the ligand are conserved in NR2A NTD (but not in NR2C or NR2D NTD). Out of 13 contacting residues, 11 are identical between the two subunits, one is homologous (T233 which is a serine in NR2A) and one is absent (V42 which is a glycine in NR2A) (Figure 1). The question arises then of why ifenprodil does not affect activity of NR1/NR2A receptors by binding to NR2A NTD as the zinc ion does. A single residue could make the difference. For instance, it is conceivable that ifenprodil cannot enter the NR2A NTD crevice because of steric hindrance produced by a bulky NR2A-specific residue protruding in the crevice. A potential candidate residue is NR2A-H42 which is replaced by a serine in NR2B. However, substituting this histidine into a shorter alanine does not confer ifenprodil sensitivity (LM and PP, unpublished observation). The most divergent region between NR2A and NR2B NTD is the  $\beta$ 1- $\alpha$ 1 region, which includes NR2B-V42. Again, replacing this entire region of NR2A-NTD by that of NR2B fails to confer ifenprodil sensitivity to the modified NR1/NR2A receptor (LM and PP, unpublished observation). Functional studies using NTD chimeric NR2 subunits and binding studies on the isolated NR2B NTD (Perin-Dureau et al., 2002; Wong et al., 2005) indicate that the molecular determinants underlying high-affinity ifenprodil binding are fully embedded in the NR2B NTD with no contribution from NR2B-specific residues outside this domain. It is therefore possible that ifenprodil selectivity for NR2B NTD originates from a limited number of NR2B-specific residues scattered throughout the NTD sequence and that are key for correct positioning of residues directly interacting with the ifenprodil molecule.

MOL #50971

## Acknowledgments

We thank Sanofi-Synthélabo for the gift of ifenprodil.

MOL #50971

## References

Acher FC and Bertrand HO (2005) Amino acid recognition by Venus flytrap domains is encoded in an 8-residue motif. *Biopolymers* **80**:357-66.

Alarcon K, Martz A, Mony L, Neyton J, Paoletti P, Goeldner M and Foucaud B (2008) Reactive derivatives for affinity labeling in the ifenprodil site of NMDA receptors. *Bioorg. Med. Chem. Lett.* **18**:2765-2770.

Avenet P, Léonardon J, Besnard F, Graham D, Frost J, Deporteere H, Langer SZ and Scatton B (1996) Antagonist properties of the stereoisomers of ifenprodil at NR1A/NR2A and NR1A/NR2B subtypes of the NMDA receptor expressed in *Xenopus* oocytes. *Eur. J. Pharmacol.* **296**:209-213.

Barnum D, Greene J, Smellie A and Sprague P (1996) Identification of common functional configurations among molecules. *J. Chem. Inf. Comput. Sci.* **36**:563-571.

Bertrand HO, Bessis AS, Pin JP and Acher FC (2002) Common and selective molecular determinants involved in metabotropic glutamate receptor agonist activity. *J. Med. Chem.* **45**:3171-3183.

Brooks BR, Bruccoleri RE, Olafson DJ, States DJ, Swaminathan S and Karplus M (1983) CHARMM: A Program for Macromolecular Energy, Minimization, and Dynamics Calculations. *J. Comput. Chem.* **4**:187-217.

Chazot PL (2004) The NMDA receptor NR2B subunit: A valid therapeutic target for multiple CNS pathologies. *Curr. Med. Chem.* **11**:389-396.

Chenard BL and Menniti FS (1999) Antagonists Selective for NMDA Receptors Containing the NR2B subunit. *Curr. Pharm. Des.* **5**:381-404.

Chizh BA, Headley PM and Tzschentke TM (2001) NMDA receptor antagonists as analgesics: focus on the NR2B subtype. *Trends Pharmacol. Sci.* **22**:636-642.

Choi YB and Lipton SA (1999) Identification and mechanism of action of two histidine residues underlying high-affinity Zn<sup>2+</sup> inhibition of the NMDA receptor. *Neuron* **23**:171-180.

Cull-Candy SG and Leszkiewicz DN (2004) Role of Distinct NMDA Receptor Subtypes at Central Synapses. *Sci. STKE* **255**:1-9.

Dingledine R, Borges K, Bowie D and Traynelis SF (1999) The glutamate receptor ion channels. *Pharmacol. Rev.* **51**:7-61.

Foucaud B, Laube B, Schemm R, Kreimeyer A, Goeldner M and Betz H (2003) Structural model of the N-methyl-D-aspartate receptor glycine site probed by site-directed chemical coupling. *J. Biol. Chem.* **278**:24011-24017.

Foucaud B, Perret P, Grutter T and Goeldner M (2001) Cysteine mutants as chemical sensors for ligand-receptor interactions. *Trends Pharmacol. Sci.* **22**:170-173.

MOL #50971

Furukawa H and Gouaux E (2003) Mechanisms of activation, inhibition and specificity: crystal structures of the NMDA receptor NR1 ligand-binding core. *EMBO J.* **22**:2873-2885.

Gallagher MJ, Huang H, Pritchett DB and Lynch DR (1996) Interactions between ifenprodil and the NR2B subunit of the N-methyl-D-aspartate receptor. *J. Biol. Chem.* **271**:9603-9611.

Gielen M, Le Goff A, Stroebel D, Johnson JW, Neyton J and Paoletti P (2008) Structural Rearrangements of NR1/NR2A NMDA receptors during allosteric inhibition. *Neuron* **57**:80-93.

Gogas KR (2006) Glutamate-based therapeutic approaches: NR2B receptor antagonists. *Curr. Opin. Pharmacol.* **6**:68-74.

Hatton CJ and Paoletti P (2005) Modulation of triheteromeric NMDA receptors by N-terminal domain Ligands. *Neuron* **46**:261-274.

Kemp and McKernan (2002) NMDA receptor pathways as drug targets. *Nat. Neurosci.* **5**:1039-1042.

Kew JNC and Kemp JA (2005) Ionotropic and metabotropic glutamate receptor structure and pharmacology. *Psychopharmacology* **179**:4-29.

Kunishima N, Shimada Y, Tsuji Y, Sato T, Yamamoto M, Kumasaka T, Nakanishi S, Jingami H and Morikawa K (2000) Structural basis of glutamate recognition by a dimeric metabotropic glutamate receptor. *Nature* **407**:971-977.

Low CM, Zheng F, Lyuboslavsky P and Traynelis SF (2000) Molecular determinants of coordinated proton and zinc inhibition of N-methyl-D-aspartate NR1/NR2A receptors. *Proc. Nat. Acad. Sci. U. S. A.* **97**:11062-11067.

Magnusson U, Salopek-Sondi B, Luck LA and Mowbray SL (2004) X-ray structures of the leucine-binding protein illustrate conformational changes and the basis of ligand specificity. *J. Biol. Chem.* **279**:8747-8752.

Malherbe P, Mutel V, Broger C, Perin-Dureau F, Kemp JA, Neyton J, Paoletti P and Kew JNC (2003) Identification of critical residues in the amino terminal domain of the human NR2B subunit involved in the RO 25-6981 binding pocket. *J. Pharmacol. Exp. Ther.* **307**:897-905.

Marinelli L, Cosconati S, Steinbrecher T, Limongelli V, Bertamino A, Novellino E and Case DA (2007) Homology modeling of NR2B modulatory domain of NMDA receptor and analysis of ifenprodil binding. *ChemMedChem* **2**:1498-1510.

Masuko T, Kashiwagi K, Kuno T, Nguyen ND, Pahk AJ, Fukuchi J, Igarashi K and Williams K (1999) A regulatory domain (R1-R2) in the amino terminus of the N-methyl-D-aspartate receptor: Effects of spermine, protons, and ifenprodil, and structural similarity to bacterial leucine/isoleucine/valine binding protein. *Mol. Pharmacol.* **55**:957-969.

Mayer ML (2006) Glutamate receptors at atomic resolution. *Nature* **440**:456-462.

MOL #50971

Mott DD, Doherty JJ, Zhang SN, Washburn MS, Fendley MJ, Lyuboslavsky P, Traynelis SF and Dingledine R (1998) Phenylethanolamines inhibit NMDA receptors by enhancing proton inhibition. *Nat. Neurosci.* **1**:659-667.

Nikam SS and Meltzer LT (2002) NR2B selective NMDA receptor antagonists. *Curr. Pharm. Des.* **8**:845-855.

Paoletti P, Ascher P and Neyton J (1997) High-affinity Zinc inhibition of NMDA NR1-NR2A Receptors. *J. Neurosci.* **17**:5711-5725.

Paoletti P and Neyton J (2007) NMDA receptor subunits: function and pharmacology. *Curr. Opin. Pharmacol.* **7**:39-47.

Paoletti P, Perin-Dureau F, Fayyazuddin A, Goff AL, Callebaut I and Neyton J (2000) Molecular Organization of a Zinc Binding N-Terminal Modulatory Domain in a NMDA Receptor Subunit. *Neuron* **28**:911-925.

Perin-Dureau F, Rachline J, Neyton J and Paoletti P (2002) Mapping the Binding Site of the Neuroprotectant Ifenprodil on NMDA Receptors. *J. Neurosci.* **22**:5955-5965.

Pinard E, Alanine A, Bourson A, Büttelmann B, Gill R, Heitz M-P, Jaeschke G, Mutel V, Trube G and Wyler R (2001) Discovery of (R)-1-[2-Hydroxy-3-(4-hydroxy-phenyl)-propyl]-4-(4-methyl-benzyl)-piperidin-4-ol: A Novel NR1/2B Subtype Selective NMDA Receptor Antagonist. *Bioorg. Med. Chem. Lett.* **11**:2173-2176.

Rachline J, Perin-Dureau F, Goff AL, Neyton J and Paoletti P (2005) The micromolar Zinc-Binding Domain on the NMDA Receptor Subunit NR2B. *J. Neurosci.* **25**:308-317.

Rost B and Sander C (1993) Prediction of Protein Secondary Structure at Better than 70% Accuracy. *J. Mol. Biol.* **232**:584-599.

Schelkun RM, Yuen P-W, Serpa K, Meltzer LT, Wise LD, Whitemore ER and Woodward RM (2000) Subtype-selective N-Methyl-D-aspartate Receptor Antagonists: Benzimidazole and Hydantoin as Phenol Replacements. *J. Med. Chem.* **43**:1892-1897.

Tamiz AP, Whitemore ER, Zhou Z-L, Huang J-C, Drewe JA, Chen J-C, Cai S-X, Weber E, Woodward RM and Keana JF (1998) Structure-Activity Relationships for a Series of Bis(phenylalkyl)amines: Potent Subtype-Selective Inhibitors of N-Methyl-D-Aspartate Receptors. *J. Med. Chem.* **41**:3499-3506.

Venkatachalam CM, Jiang X, Oldfield T and Waldman M (2003) LigandFit: a novel method for the shape-directed rapid docking of ligands to protein active sites. *J. Mol. Graphics. Modell.* **21**:289-307.

Williams K (1993) Ifenprodil discriminates subtypes of the N-methyl-D-aspartate receptor-selectivity and mechanisms at recombinant heteromeric receptors. *Mol. Pharmacol.* **44**:851-859.

MOL #50971

Wong E, Ng FM, Yu CY, Lim P, Lim LH, Traynelis SF and Low CM (2005) Expression and characterization of soluble amino-terminal domain of NR2B subunit of N-methyl-D-aspartate receptor. *Prot. Sci.* **14**:2275-2283.

Wright JL, Gregory TF, Bigge CF, Boxer PA, Serpa K, Meltzer LT and Wise LD (1999) Subtype-selective N-Methyl-D-aspartate Receptor Antagonists: Synthesis and Biological evaluation of 1-(arylalkynyl)-4-benzylpiperidines. *J. Med. Chem.* **42**:2469-2477.

Wright JL, Gregory TF, Kesten SR, Boxer PA, Sherpa KA, Meltzer LT and Wise LD (2000) Subtype-Selective N-Methyl-D-Aspartate Receptor Antagonists: Synthesis and Biological Evaluation of 1-(Heteroarylalkynyl)-4-benzylpiperidines. *J. Med. Chem.* **43**:3408-3419.

MOL #50971

## Figure Legends

### Figure 1: Sequence alignment of NR2A and NR2B NTDs with the agonist-binding domain of mGluR1.

The indicated  $\alpha$ -helices (red) and  $\beta$ -strands (green) of mGluR1 are from the X-ray structure of the agonist-binding domain of mGluR1 (PDB 1ewk:A; Kunishima et al., 2000). Secondary structure elements of NR2A and NR2B NTDs were predicted using PROF predictions (see Methods). Yellow closed boxes correspond to residues of mGluR1 contacting the glutamate molecule in mGluR1 ABD X-ray structure (Kunishima et al., 2000), orange closed boxes to residues of NR2A controlling high-affinity zinc inhibition and to residues of NR2B controlling zinc inhibition and not ifenprodil inhibition (Paoletti et al., 2000 and Rachline et al., 2005), green closed boxes to residues of NR2B selectively controlling ifenprodil inhibition (Perin-Dureau et al., 2002), blue closed boxes to residues of NR2B controlling both ifenprodil and zinc inhibition (Rachline et al., 2005). Mutations into alanine of these highlighted NR2A and NR2B residues all result in a decrease of zinc and/or ifenprodil sensitivity, except for V42, which decreases ifenprodil sensitivity but increases zinc sensitivity (see Rachline et al., 2005). In NR2A, residues located at the entrance of the NTD central cleft, proposed as residues providing a favourable electrostatic environment for zinc to access the cleft (Paoletti et al., 2000), are depicted in orange open boxes. In NR2B, newly identified residues contacting ifenprodil in the docking models (see Results) are depicted in pink closed boxes (orientation 1) and pink open boxes (orientation 2). Note that despite the conserved pattern of secondary structure elements (alternation of  $\beta$ -strands and  $\alpha$ -helices), the sequence identity between mGluR1 ABD and NR2 (or NR2A) NTD is very low (~12%).

### Figure 2: Ifenprodil can bind NR2B NTD with two possible orientations.

- A. Orientation 1:** a) 3D model of ifenprodil binding into the NTD of NR2B in orientation 1 with ifenprodil B ring close to the entrance of the cleft and ring A contacting the interlobe hinge (see Results). The NTD  $\alpha$ -carbon backbone is displayed as a dark green ribbon. Ifenprodil is displayed as sticks (carbons and hydrogens in orange, nitrogen in dark blue and oxygens in red). b) Expanded view of the binding of ifenprodil in orientation 1, showing its interactions with residues of the NTD interlobe cleft. Non-carbon atoms are displayed as follows: hydrogens in white, nitrogens in

MOL #50971

dark blue and oxygens in red. Only polar hydrogens and hydrogens of threonine methyl groups are represented. Residues selectively controlling ifenprodil inhibition (Perin-Dureau et al., 2002) are displayed with light green carbon chains, and residues controlling both ifenprodil and zinc inhibition (Rachline et al., 2005) with light blue carbon chains. Residues displayed with pink carbon chains represent newly identified residues contacting ifenprodil in the model, and for which mutagenesis data were lacking. H-bonds are displayed as red dotted lines and coulombian interactions as red plain lines. At the bottom of the figure is displayed E236 (green), a residue that, in the model, is important for positioning T233 (see Results). Note also that L261 (located next to V262), a residue selectively controlling ifenprodil inhibition and contacting ifenprodil in this model is not represented for clarity reasons. **c)** Ifenprodil binding-pocket. Schematic 2D-view of the interactions of ifenprodil in orientation 1 with residues of NR2B NTD (same colour code as in Figure 1Ab). Van der Waals interactions are displayed as black dotted lines, H-bonds as red dotted lines and coulombian interactions as red plain lines.

**B. Orientation 2:** The representation conventions used are the same as in Figure 1A. **a)** 3D model of ifenprodil binding into the NTD of NR2B in orientation 2: ring B contacts the interlobe hinge while ring A is close to the entrance of the binding cleft. As in Figure 1A, L261 is not displayed for clarity reasons. **b)** Expanded view of the binding of ifenprodil in orientation 2, showing its interactions with residues of the NTD interlobe cleft. **c)** The ifenprodil binding-pocket. Schematic 2D-view of the interactions of ifenprodil in orientation 2 with the residues of NR2B NTD.

**Figure 3: The conformations adopted by ifenprodil in orientations 1 and 2 are likely to be bioactive conformations.**

**A.** Pharmacophore model of ifenprodil-like antagonists binding to NR2B NTD. Pharmacophore models are 3D arrangements of electronic features, each feature representing an interaction of the ligand with its receptor. Each feature is symbolised by a central ball representing the application center of the feature in the ligand, surrounded by a tolerance sphere (light blue for hydrophobic features, red for positive ionisable and orange for hydrogen bond donors). As H-bonds are directional interactions, the H-bond feature is represented by two balls linked by an arrow which indicates the direction from the heavy atom to the projected point representing the position from which the hydrogen will extend. **B and C.**

MOL #50971

Mapping of orientation 1 (B) and orientation 2 (C) ifenprodil conformations to the pharmacophore model shown in A. Ifenprodil is represented as sticks, with carbons in grey, hydrogens in white, oxygens in red and nitrogen in dark blue. Ifenprodil in both orientations 1 and 2 closely fits the pharmacophore model (fit value of 2.34 and 2.85 over 4, respectively).

**Figure 4: NR2B-V262, a new key residue selectively controlling ifenprodil inhibition.**

**A.** Typical current traces obtained from oocytes co-expressing the wt NR1 subunit with wt or mutated V262I, V262F or V262D NR2B subunits. Ifenprodil was applied at a concentration of 300 nM and zinc at 1  $\mu$ M, each during an application of agonists. The bars above the current traces indicate the duration of agonists, ifenprodil, and zinc applications. Note that the inhibition produced by 1  $\mu$ M zinc is only weakly affected by any of the three mutations (inhibition of  $54 \pm 8$  % [n = 3],  $41 \pm 2$  % [n = 4] and  $51 \pm 2$  % [n = 3] for NR2B-V262I, V262F and V262D mutations, respectively, vs  $61 \pm 4$  % for wt receptors [n = 12]). In contrast, ifenprodil sensitivity is strongly reduced by the NR2B-V262F or D mutations while it is slightly increased with the NR2B-V262I mutation.

**B.** Ifenprodil (left) and zinc (right) concentration-response curves of NR1/NR2B receptors containing different substitutions at the NR2B-V262 position. The dashed curves are the fits of the ifenprodil or zinc dose-response curves of wt NR1/NR2B receptors (short dashes) and receptors truncated for their entire NR2B-NTD (NR1/NR2B- $\Delta$ NTD, long dashes; see Rachline et al., 2005). Experimental data points obtained with NR1/NR2B- $\Delta$ NTD receptors are displayed as closed diamonds. Each data point is the mean value of at least three different cells. The estimated values of IC<sub>50</sub> are listed in Table 1. Note that NR2B-V262 mutations selectively and differentially affect ifenprodil sensitivity. Note also that the experimental data points and the fits of the NR1/NR2B-V262D (closed triangles) and NR1/NR2B-V262F (open triangles) mutant receptor dose-response curves overlap.

**Figure 5: NR2B-Y231, an additional key residue controlling ifenprodil inhibition.**

Ifenprodil and zinc sensitivity of NR1/NR2B receptors substituted with different residues at the NR2B-Y231 position. In each panel, the dashed curves are the fits of the ifenprodil or zinc dose-response curves of wt NR1/NR2B receptors (short dashes) and NR1/NR2B- $\Delta$ NTD receptors (long dashes). Each data point is the mean value of at least three different oocytes.

**A.** Ifenprodil concentration-response curves **B.** Zinc concentration-response curves. The

MOL #50971

estimated values of  $IC_{50}$  are listed in Table 1. Note that the shift in ifenprodil sensitivity produced by the NR2B-Y231A mutation is almost as large as the shift produced by the deletion of the entire NR2B NTD (dashed line).

**Figure 6: Effects of NR2B-D206 and NR2B-T76 mutations on ifenprodil and zinc sensitivity**

Ifenprodil and zinc sensitivity of NR1/NR2B receptors substituted with different residues at NR2B-D206 and NR2B-T76 positions. In each panel, the dashed curves are the fits of the ifenprodil or zinc dose-response curves of wt NR1/NR2B receptors (short dashes) and NR1/NR2B- $\Delta$ NTD receptors (long dashes). Each data point is the mean value of at least three different oocytes. **A.** Ifenprodil concentration-response curves of NR1/NR2B receptors mutated at the NR2B-D206 position. **B.** Zinc concentration-response curves of NR1/NR2B receptors mutated at the NR2B-D206 position. **C.** Ifenprodil concentration-response curves of NR1/NR2B receptors mutated at the NR2B-T76 position. **D.** Zinc concentration-response curves of NR1/NR2B receptors mutated at the NR2B-T76 position. The estimated values of  $IC_{50}$  are listed in Table 1.

**Figure 7: Orienting ifenprodil in its binding pocket using cysteine affinity labelling**

**A.** Principle of the cysteine affinity labelling approach. This technique is based on the formation of a covalent bound between a cysteine-reactive ligand (schematised in orange with a red circle representing the cysteine-reactive group) and a cysteine-modified receptor (schematised in green). If the cysteine and the cysteine-reactive group are in close proximity, the formation of a covalent bound leads to an irreversible labelling of the receptor (in our case an irreversible inhibition). In the present work, we used molecule **4**, a cysteine-reactive ifenprodil analogue containing a cysteine-reactive chloroacetamide group on the para-position of the B-ring (circled in red). **B.** Affinity labelling results. For each position,  $I_{incub}/I_0$  ratio of the cysteine mutant is represented as a red bar and that of the corresponding alanine mutant as a grey bar. Error bars represent the standard error of the mean. The numbers of oocytes used for each construction are shown in parenthesis above the bars. We used a student T-test to probe for a significant difference between the  $I_{incub}/I_0$  ratios of the alanine and the cysteine substitution at the same position (\*:  $P < 0.05$ ). **C.** Representation of molecule **4** (orange sticks) bound to the NR2B NTD in orientation 1, with cysteine residues at positions NR2B-

## MOL #50971

T76, D206 (pink carbon chains) and L205 (grey carbon chain) introduced by *in silico* mutagenesis. Sulfur atoms are displayed in yellow and hydrogen atoms in white. Hydrogen atoms of the cysteine carbon chains are not represented. The chloroacetamide group (displayed as sticks colored as follows: carbons in grey, hydrogens in white, nitrogens in dark blue and oxygens in red) displays rotational mobility (red curved arrow) and thus can potentially make covalent bonds with either lobe I (T76C) or lobe II (D206C and L205C) residues.

MOL #50971

**Table 1: Effects on ifenprodil and zinc sensitivity of various mutations in NR2B NTD**

| NR2B mutants        | ifenprodil            |                 |   | zinc                  |                 |    |
|---------------------|-----------------------|-----------------|---|-----------------------|-----------------|----|
|                     | IC <sub>50</sub> (μM) | mutant/wt ratio | n | IC <sub>50</sub> (μM) | mutant/wt ratio | n  |
| wt                  | 0.16 ± 0.01           |                 | 9 | 0.70 ± 0.08           |                 | 15 |
| <b>T76</b>          |                       |                 |   |                       |                 |    |
| T76A                | 2.3 ± 0.8             | 15              | 3 | 0.60 ± 0.06           | 0.8             | 6  |
| T76C                | 2.5 ± 0.1             | 16              | 3 | 0.9 ± 0.1             | 1.3             | 3  |
| T76S                | 0.43 ± 0.01           | 2.8             | 3 | 0.40 ± 0.05           | 0.6             | 3  |
| <b>D77</b>          |                       |                 |   |                       |                 |    |
| D77C                | 2.8 ± 0.2             | 18              | 4 | 0.9 ± 0.3             | 1.3             | 5  |
| <b>Q153</b>         |                       |                 |   |                       |                 |    |
| Q153A               | 0.22 ± 0.04           | 1.4             | 7 | 0.8 ± 0.3             | 1.1             | 4  |
| Q153C               | 0.28 ± 0.02           | 1.8             | 7 | 0.8 ± 0.3             | 1.1             | 6  |
| <b>D206</b>         |                       |                 |   |                       |                 |    |
| D206A               | 4 ± 1                 | 30              | 7 | 2.6 ± 0.4             | 3.7             | 6  |
| D206C               | 5 ± 2                 | 30              | 4 | 1.4 ± 0.1             | 2.0             | 5  |
| D206E               | 1.5 ± 0.1             | 10              | 8 | 0.74 ± 0.02           | 1.1             | 6  |
| D206F               | 7 ± 4                 | 45              | 3 | 2.0 ± 0.1             | 2.9             | 3  |
| D206K               | 13 ± 15               | 80              | 3 | 4.7 ± 0.2             | 6.7             | 3  |
| <b>Y231</b>         |                       |                 |   |                       |                 |    |
| Y231A               | 53 ± 10               | 350             | 3 | 1.6 ± 0.4             | 2.3             | 3  |
| Y231C               | 26 ± 8                | 170             | 6 | 1.6 ± 0.6             | 2.3             | 6  |
| <b>V262</b>         |                       |                 |   |                       |                 |    |
| V262A               | 0.41 ± 0.04           | 2.6             | 3 | 0.9 ± 0.1             | 1.3             | 3  |
| V262C               | 0.35 ± 0.03           | 2               | 3 | 0.7 ± 0.1             | 1.0             | 4  |
| V262D               | 8 ± 2                 | 50              | 4 | 0.9 ± 0.1             | 1.3             | 3  |
| V262F               | 8 ± 2                 | 50              | 3 | 1.6 ± 0.3             | 2.3             | 4  |
| V262G               | 0.87 ± 0.04           | 5.6             | 5 | 1.2 ± 0.3             | 1.7             | 3  |
| V262I               | 0.09 ± 0.001          | 0.55            | 5 | 0.9 ± 0.1             | 1.3             | 3  |
| <b>Y282</b>         |                       |                 |   |                       |                 |    |
| Y282C               | 0.8 ± 0.2             | 5               | 9 | 0.7 ± 0.1             | 1               | 7  |
| Y282S               | 0.7 ± 0.1             | 4.5             | 3 | 1.6 ± 0.6             | 2.3             | 3  |
| Y282W               | 0.24 ± 0.02           | 1.5             | 4 | 0.9 ± 0.1             | 1.3             | 3  |
| <b>NTD deletion</b> |                       |                 |   |                       |                 |    |
| NR2B-ΔNTD           | 145 ± 3               | 900             | 3 | 11 ± 1                | 16              | 3  |

(lobe I) β2

|        |  |
|--------|--|
| mGlu1  | RSVARMGDG <b>VIIGALF</b> SVHHQPPAEK <b>VP</b> ERKCGEIRE <b>QYGI</b> QRVEAMFHTL <b>DKINAD</b> PVLLPNITL <b>GSEIR</b> DC <b>SW</b> HSSVA 115 |
| NR2A   | AAAEKGPP <b>ALNI</b> AVLLG-----HSH <b>DV</b> TERELRNLWGPEQATG--LPLDV <b>NVV</b> ALLMNR-- <b>TD</b> PKSL 82                                 |
| NR2B   | RS-QKSPP <b>SIGIA</b> VIL <b>V</b> -----G <b>TS</b> D <b>VA</b> IKDAHEKDDFFHLS---VVP-- <b>RVEL</b> VAMNE-- <b>TD</b> PKSI 81               |
| N°NR2B | residues 42 43 47 76   |

(lobe I) Hinge

|        |  |
|--------|--|
| mGlu1  | <b>α2</b> LEQ <b>SIE</b> FIR-KP- <b>IAG</b> VIGPG- <b>SS</b> - <b>SVAIQVQ</b> NLLQLF-DI <b>PQ</b> IAYS- <b>AT</b> S <b>SID</b> LSDKTLYKY <b>FLR</b> VVPS <b>DT</b> LQARAM <b>LDI</b> 218                               |
| NR2A   | <b>ITH</b> VC <b>DL</b> M-SGARI <b>HGL</b> VFG <b>DD</b> TD <b>Q</b> E <b>AVA</b> QMLDFISSQTFI <b>PIL</b> GI <b>HG</b> GAS <b>MIM</b> ADKDP <b>TST</b> FF <b>Q</b> FGAS <b>IQQ</b> QAT <b>VML</b> KI 161               |
| NR2B   | <b>ITR</b> IC <b>DL</b> M-SDR <b>KIQ</b> GV <b>FAD</b> DT <b>Q</b> E <b>AIA</b> QILDFISAQ <b>TL</b> TP <b>IL</b> GI <b>HG</b> GSS <b>MIM</b> ADKDESS <b>MF</b> Q <b>F</b> GP <b>SE</b> Q <b>Q</b> AS <b>VML</b> NI 160 |
| N°NR2B | residues 101 106 127 150   |

(lobe II)

|        |  |
|--------|--|
| mGlu1  | <b>β6</b> <b>VK</b> RY <b>NW</b> TY <b>V</b> SA <b>VH</b> TE <b>GN</b> Y <b>G</b> ES <b>GMD</b> AF <b>KELAA</b> Q <b>EGL</b> CT <b>AH</b> SD <b>KI</b> Y-S <b>NAG</b> - <b>EKS</b> F <b>DR</b> LL <b>RKL</b> R <b>ERL</b> PKAR <b>VV</b> VC <b>FCE</b> GM <b>TV</b> 296                    |
| NR2A   | <b>MQ</b> DY <b>DW</b> H <b>V</b> FS <b>LV</b> TT <b>IF</b> PGY <b>RF</b> I <b>S</b> F <b>IK</b> TT <b>VD</b> NS <b>FV</b> GD <b>MD</b> Q <b>NV</b> ITL <b>DT</b> S--- <b>FED</b> AK <b>TQ</b> V <b>QL</b> KK-I-H <b>SS</b> V <b>LL</b> Y <b>CS</b> K <b>DEA</b> 236                       |
| NR2B   | <b>MEE</b> Y <b>DW</b> Y <b>IF</b> S <b>IV</b> TT <b>IF</b> PGY <b>QD</b> E <b>VN</b> K <b>IR</b> ST <b>IE</b> NS <b>FV</b> GD <b>WE</b> LE <b>EV</b> LL <b>LD</b> MS-L <b>DD</b> GD <b>S</b> K <b>I</b> Q <b>N</b> Q <b>L</b> KK-L-Q <b>SP</b> I <b>L</b> LI <b>Y</b> CT <b>KEE</b> A 237 |
| N°NR2B | residues 176 182 206 233   |

(lobe II) Hinge (lobe I)

|        |  |
|--------|--|
| mGlu1  | <b>α8</b> <b>RGL</b> LS <b>AM</b> RR <b>L</b> GV <b>GE</b> - <b>F</b> SL <b>IG</b> -- <b>SD</b> GW <b>ADR</b> DE <b>VI</b> EG <b>YE</b> VE <b>ANG</b> GI <b>TI</b> KL <b>Q</b> SP <b>EV</b> RS <b>FDD</b> Y <b>FL</b> KL <b>R</b> LD <b>TN</b> TR <b>NPW</b> F <b>PE</b> FW <b>Q</b> 373 |
| NR2A   | <b>VL</b> IL <b>SE</b> AR <b>SL</b> GL <b>TG</b> YD <b>FF</b> W <b>IV</b> PS <b>LV</b> -- <b>S</b> GN <b>T</b> EL <b>IP</b> KE <b>FPS</b> -- <b>GL</b> IS <b>V</b> SY <b>DD</b> WD-- 285   |
| NR2B   | <b>TY</b> IF <b>EV</b> AN <b>S</b> V <b>GL</b> T <b>G</b> Y <b>G</b> Y <b>TW</b> IV <b>PS</b> LV-- <b>AG</b> DT <b>D</b> IV <b>P</b> SE <b>FPT</b> -- <b>GL</b> IS <b>V</b> SY <b>D</b> EWD-- 286  |
| N°NR2B | residues 261 282   |

(lobe I) α11

|       |   |
|-------|---|
| mGlu1 | <b>HR</b> F <b>QC</b> RL <b>PG</b> H <b>LL</b> EN <b>PN</b> F <b>K</b> VC <b>T</b> GN <b>ES</b> LE <b>EN</b> Y <b>V</b> Q <b>DS</b> <b>K</b> MG <b>F</b> V <b>INA</b> I <b>Y</b> AM <b>AH</b> GL <b>Q</b> N <b>MH</b> HAL <b>C</b> -- <b>P</b> GH <b>V</b> GL <b>C</b> - <b>DAM</b> - <b>KPI</b> - <b>DGR</b> 448 |
| NR2A  | ----- <b>YS</b> LE <b>AR</b> VR <b>D</b> GL <b>G</b> IL <b>T</b> TA <b>AS</b> S <b>ML</b> E <b>K</b> FS <b>Y</b> IP <b>EAK</b> AS <b>C</b> Y <b>G</b> Q <b>AE</b> K <b>P</b> ET <b>PL</b> H 332   |
| NR2B  | ----- <b>Y</b> GL <b>P</b> AR <b>VR</b> D <b>G</b> IA <b>IT</b> TA <b>AS</b> D <b>ML</b> SE <b>HS</b> FI <b>PE</b> PK <b>SS</b> C <b>YN</b> THE <b>K</b> R <b>IY</b> Q <b>SN</b> 333  |

(lobe I) Hinge (lobe II)

|       |  |
|-------|--|
| mGlu1 | <b>α12</b> <b>KLL</b> D <b>FL</b> I <b>K</b> SS <b>SV</b> GV <b>S</b> GE <b>EV</b> W <b>F</b> DE <b>K</b> G-D <b>AP</b> GR <b>YD</b> IM <b>NL</b> Q <b>Y</b> TE <b>AN</b> RY <b>DY</b> V <b>H</b> V <b>GT</b> W <b>H</b> EG <b>V</b> LN <b>ID</b> DY <b>KI</b> 512                         |
| NR2A  | <b>TL</b> H <b>Q</b> F <b>M</b> V <b>N</b> VT <b>W</b> -- <b>D</b> G <b>K</b> D <b>LS</b> F <b>TE</b> E <b>G</b> Y <b>Q</b> V <b>H</b> PR <b>LV</b> V <b>IV</b> L <b>N</b> KD-- <b>R</b> E-- <b>W</b> E <b>K</b> V <b>G</b> K <b>W</b> EN <b>Q</b> TL <b>SL</b> R <b>H</b> AV <b>W</b> 390 |
| NR2B  | <b>ML</b> N <b>RY</b> L <b>IN</b> V <b>T</b> F-- <b>E</b> GR <b>N</b> LS <b>F</b> SE <b>D</b> G <b>Y</b> Q <b>M</b> HP <b>K</b> L <b>V</b> I <b>IL</b> LN <b>KE</b> -- <b>R</b> K-- <b>W</b> ER <b>V</b> G <b>K</b> W <b>K</b> DK <b>SL</b> Q <b>M</b> K <b>Y</b> V <b>W</b> 391           |

- Residues contacting glutamate in the agonist-binding domain of mGluR1
- Residues controlling zinc inhibition in NR2A and selectively controlling zinc inhibition in NR2B
- Residues located at the entrance of the cleft and facilitating zinc binding in NR2A NTD
- Residues selectively controlling ifenprodil inhibition
- Residues controlling both zinc and ifenprodil inhibition in NR2B
- New residues contacting ifenprodil in the orientation 1 model
- New residues contacting ifenprodil in the orientation 2 model

Figure 1

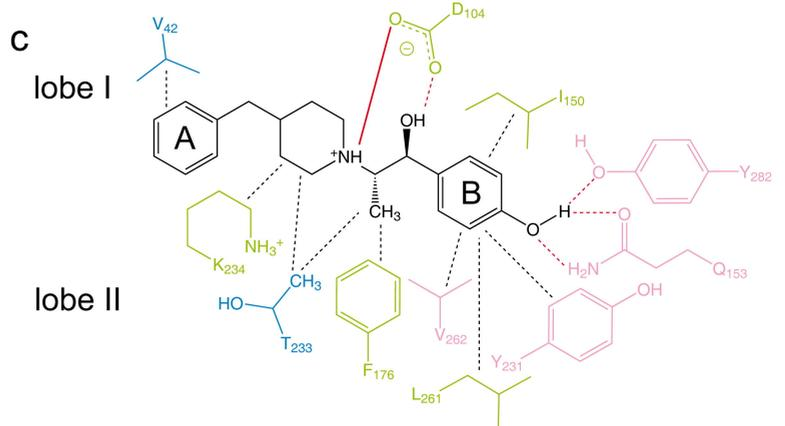
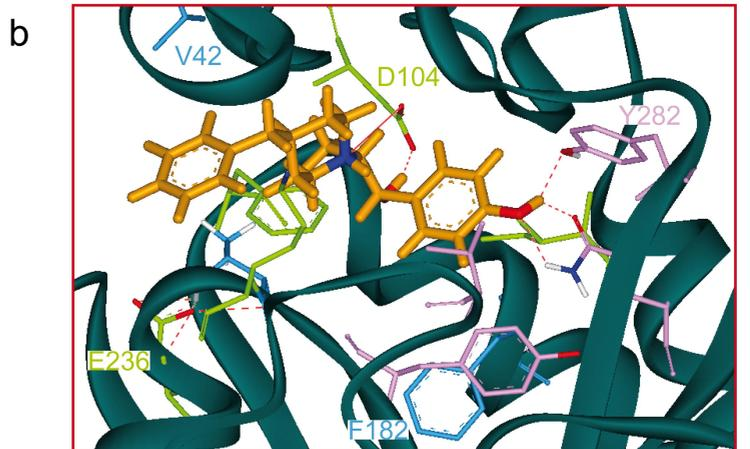
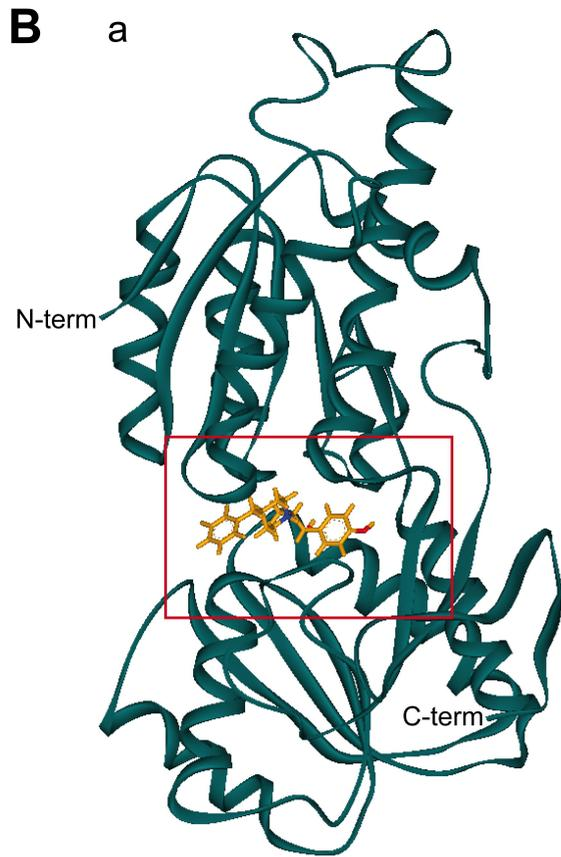
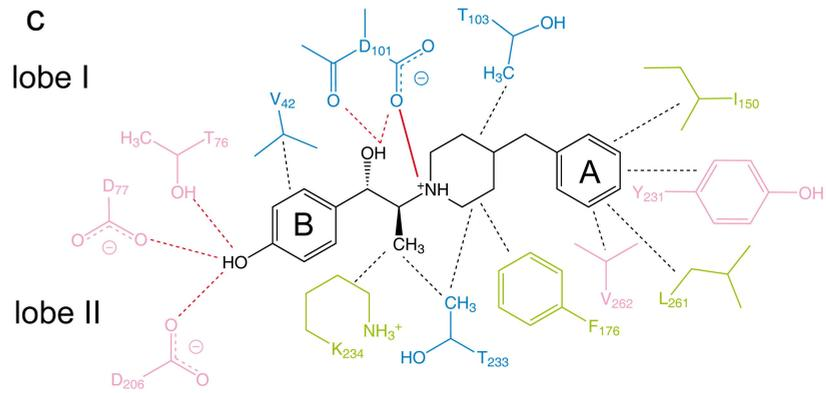
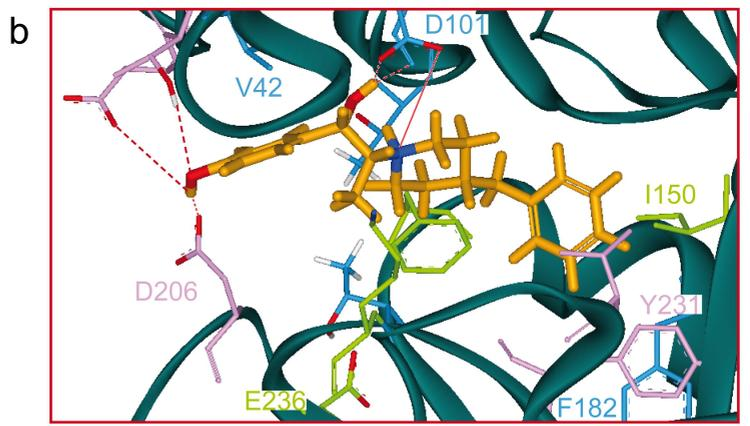
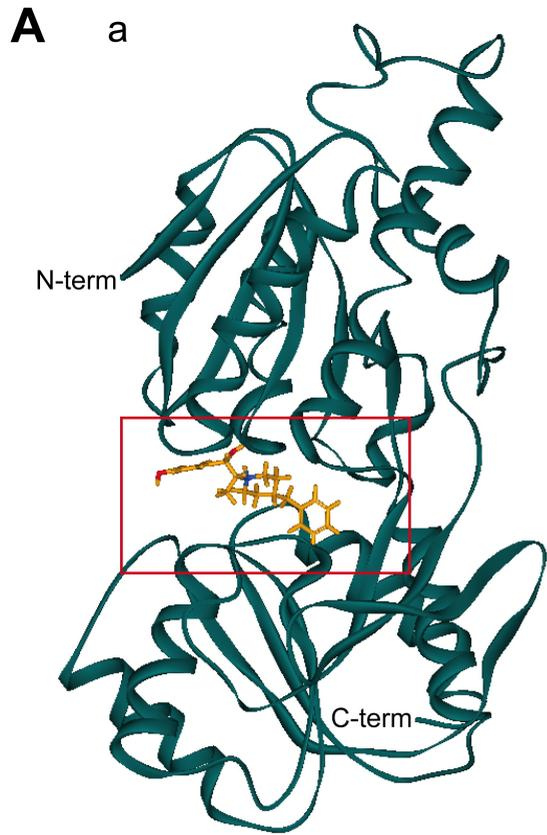
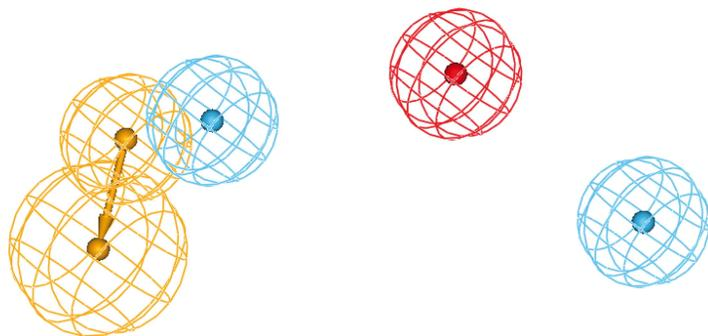
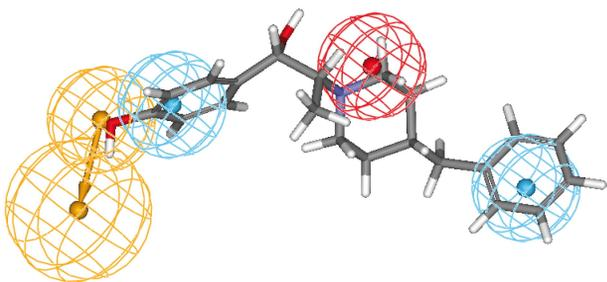
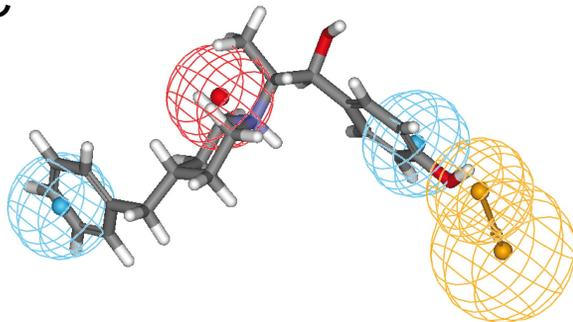


Figure 2

**A**

● hydrophobic aromatic      ● positive ionisable  
●—● H-bond donor

**B****C****Figure 3**



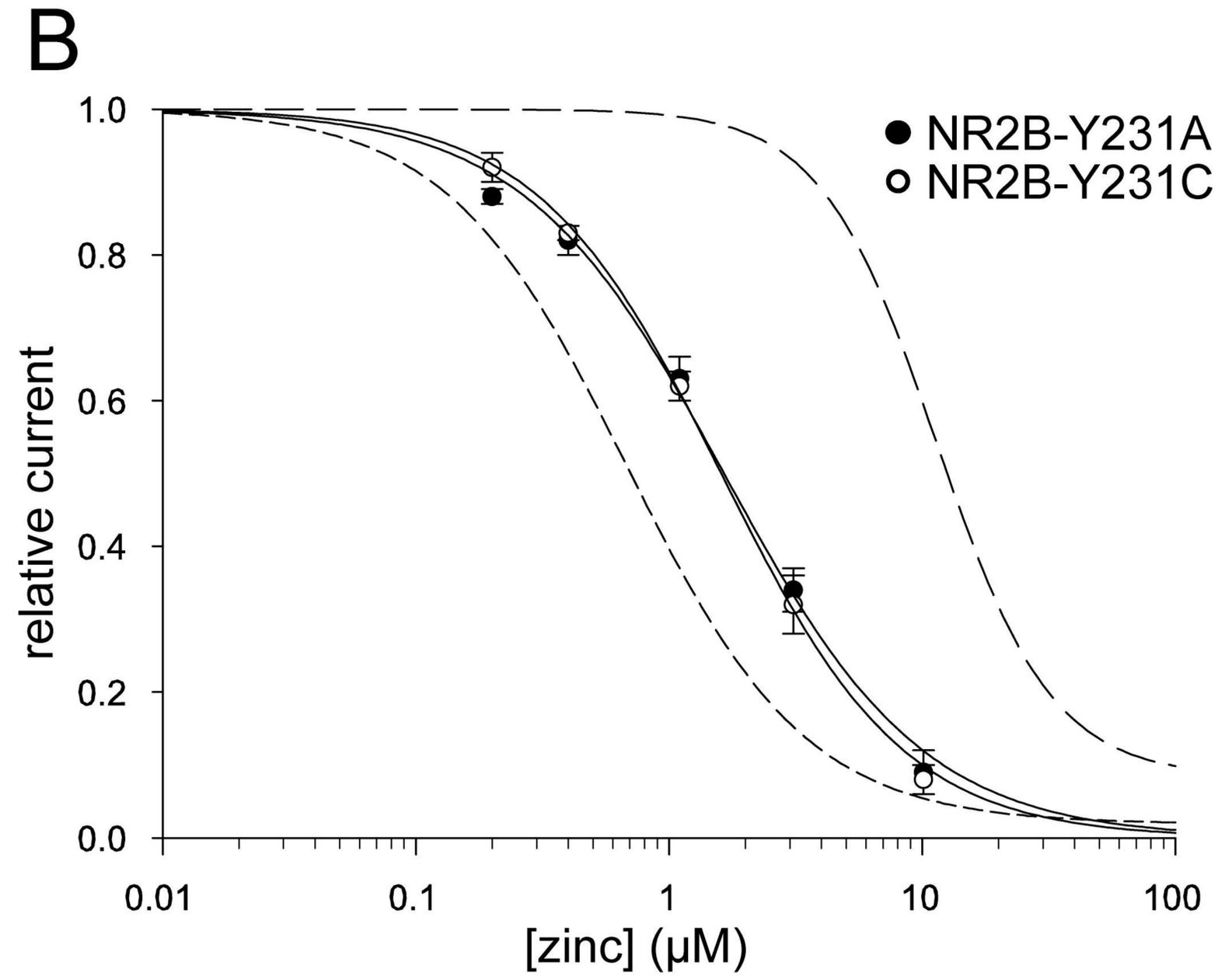
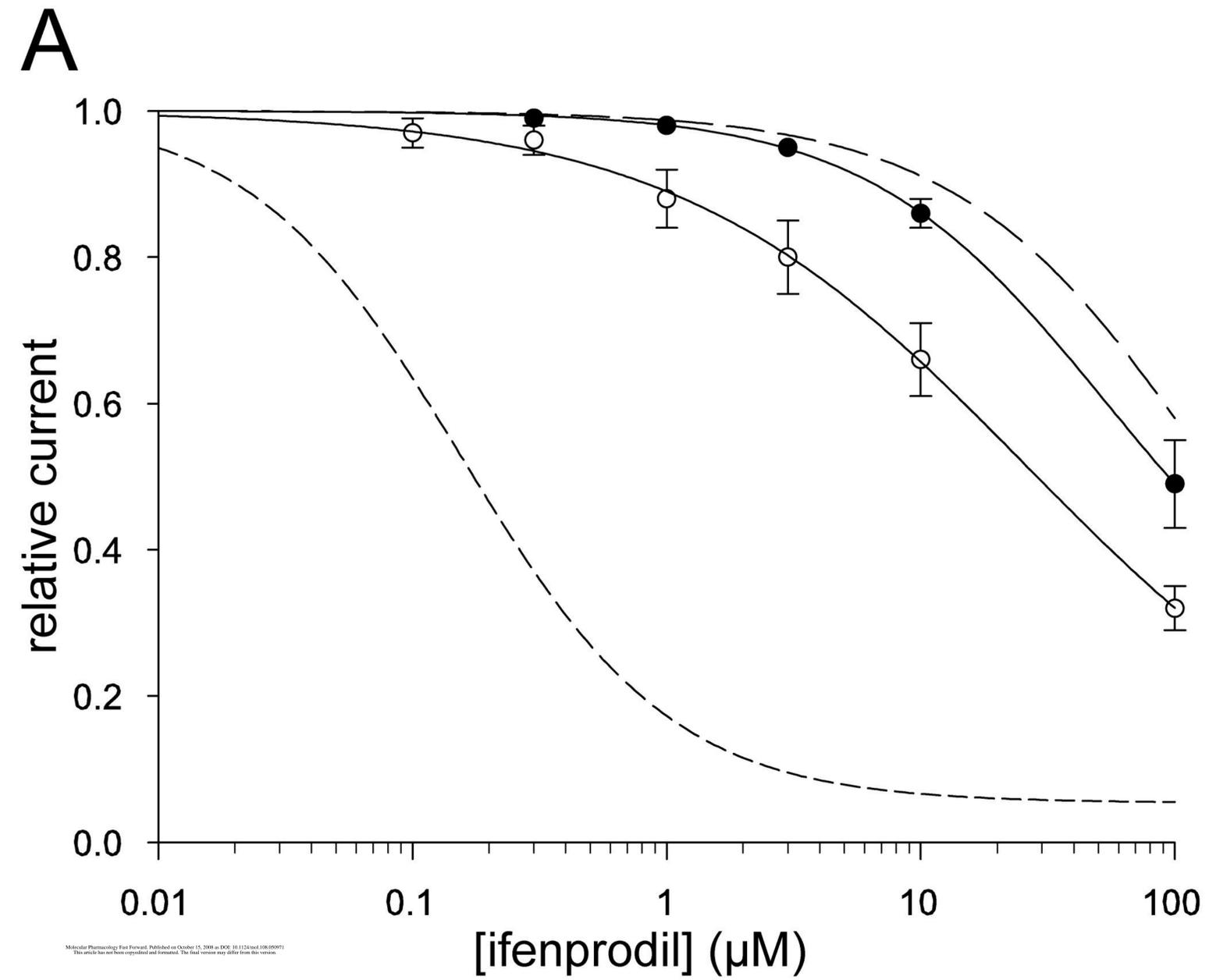
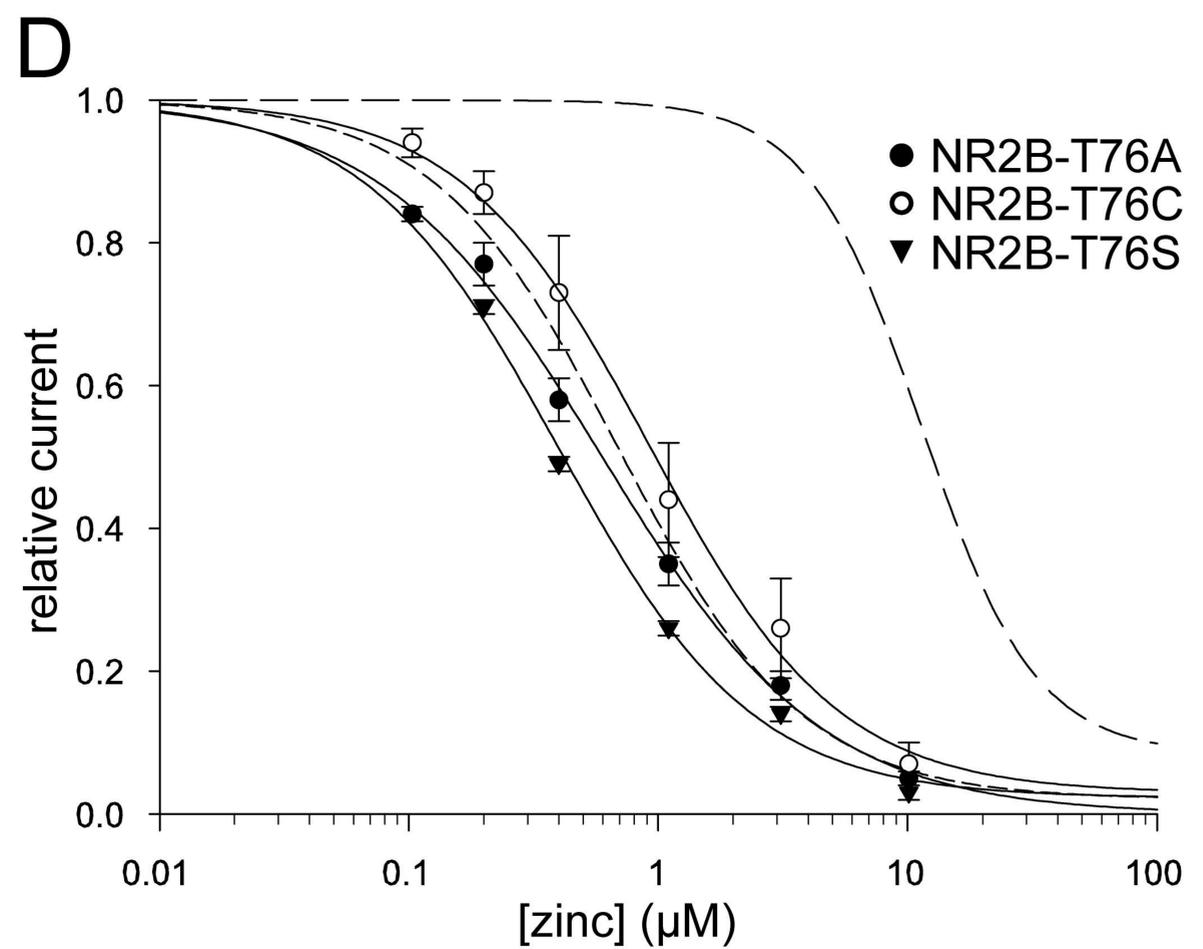
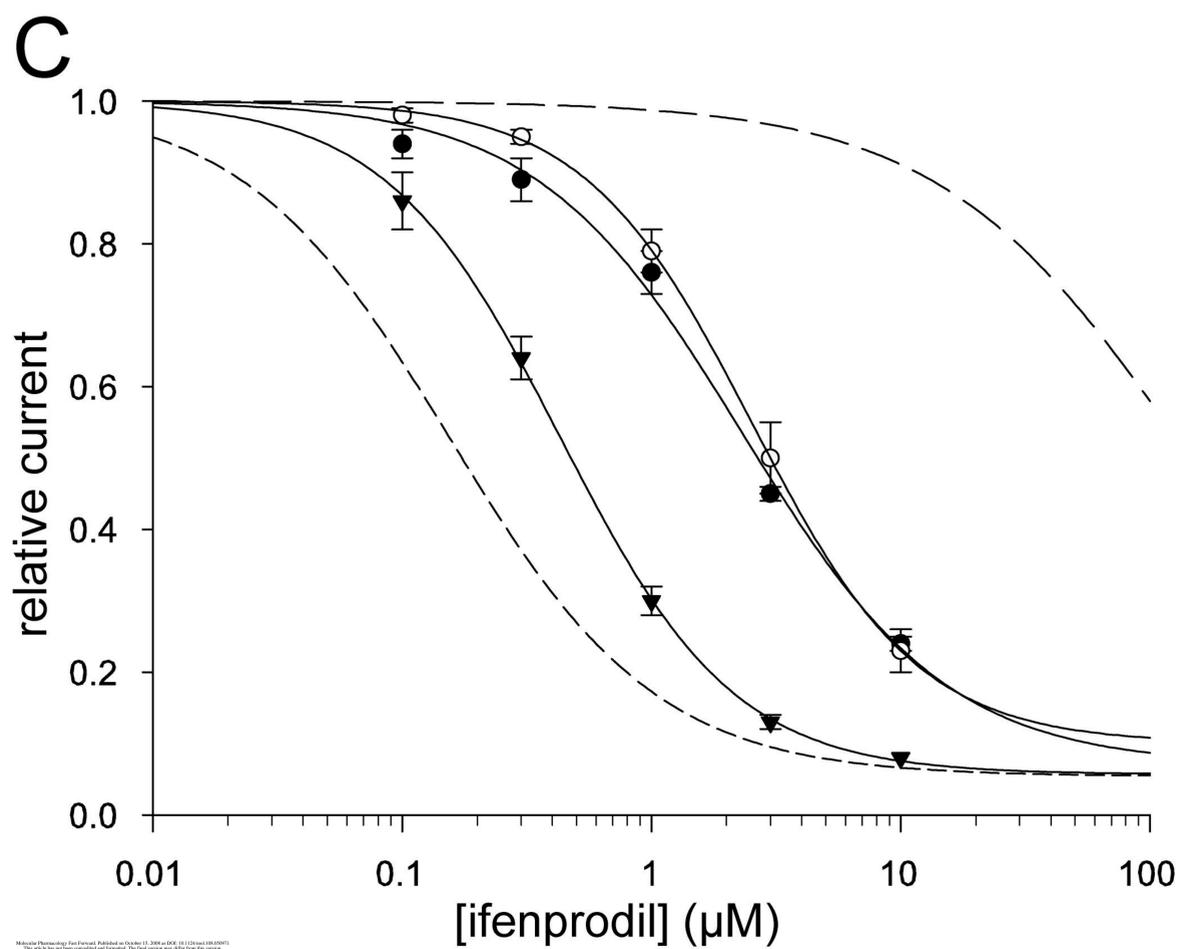
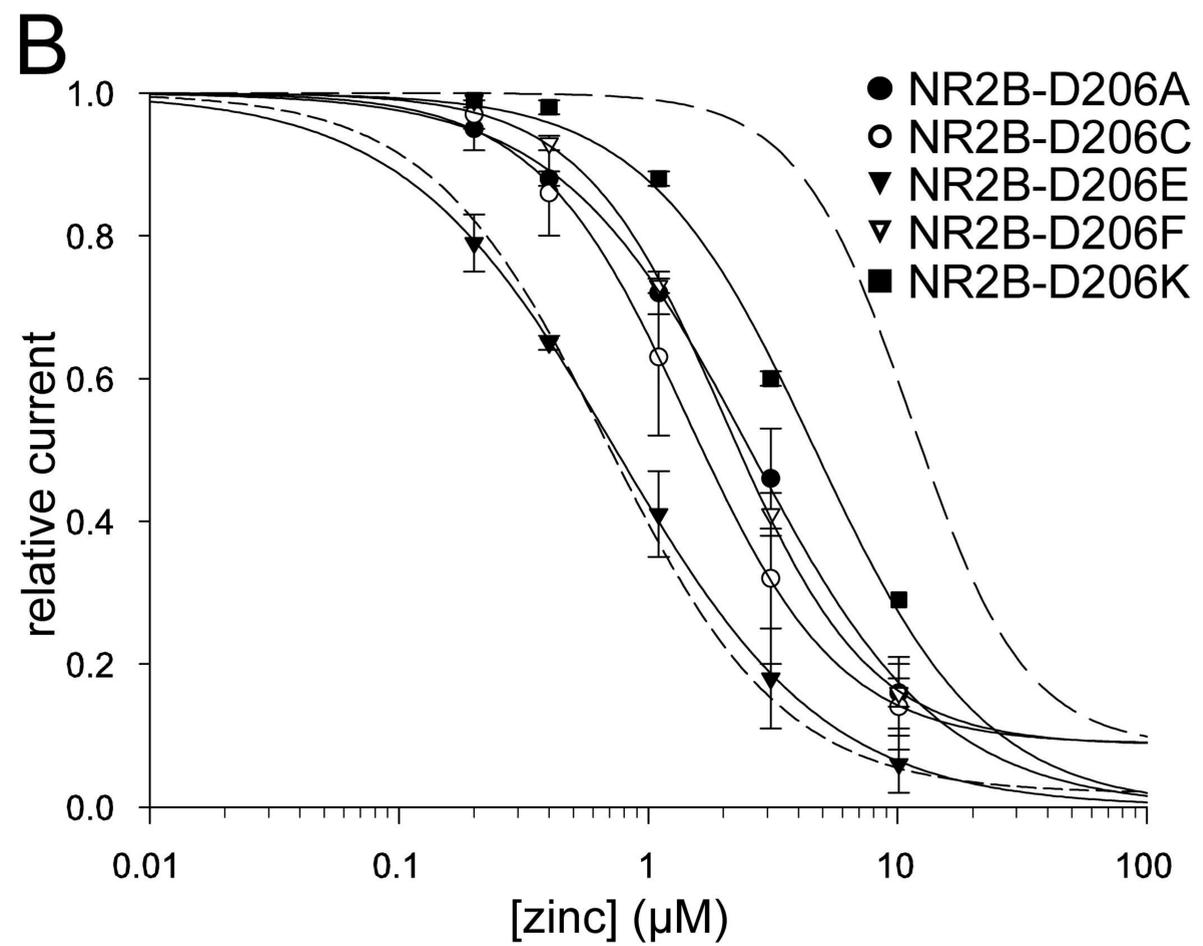
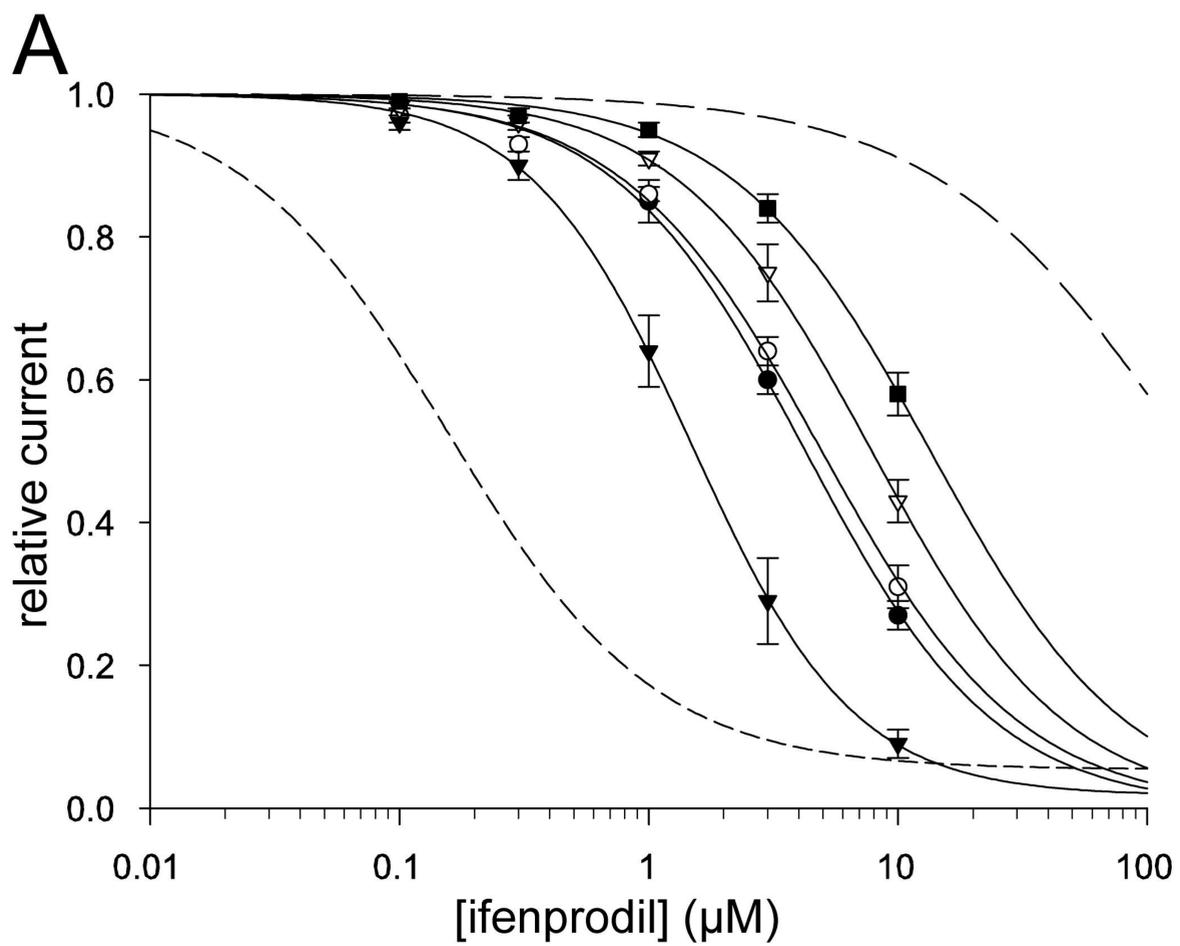


Figure 5



Molecular Pharmacology Fast Forward. Published on October 11, 2006 as DOI: 10.1124/mp.f.105.90971  
This article has not been certified by peer review. The copyright holder for this article (which was not certified by peer review) is the author/funder, who has granted bioRxiv a license to display the preprint in perpetuity. It is made available under aCC-BY-NC-ND 4.0 International license.

10.1124/mp.f.105.90971

Figure 6

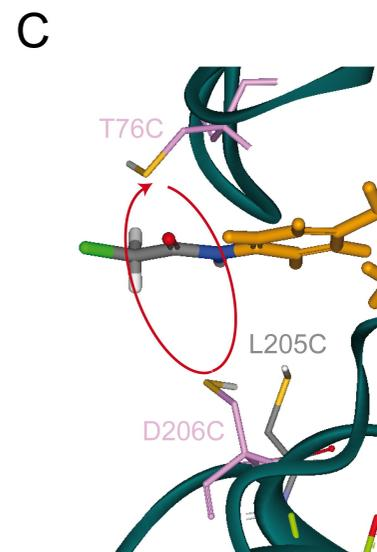
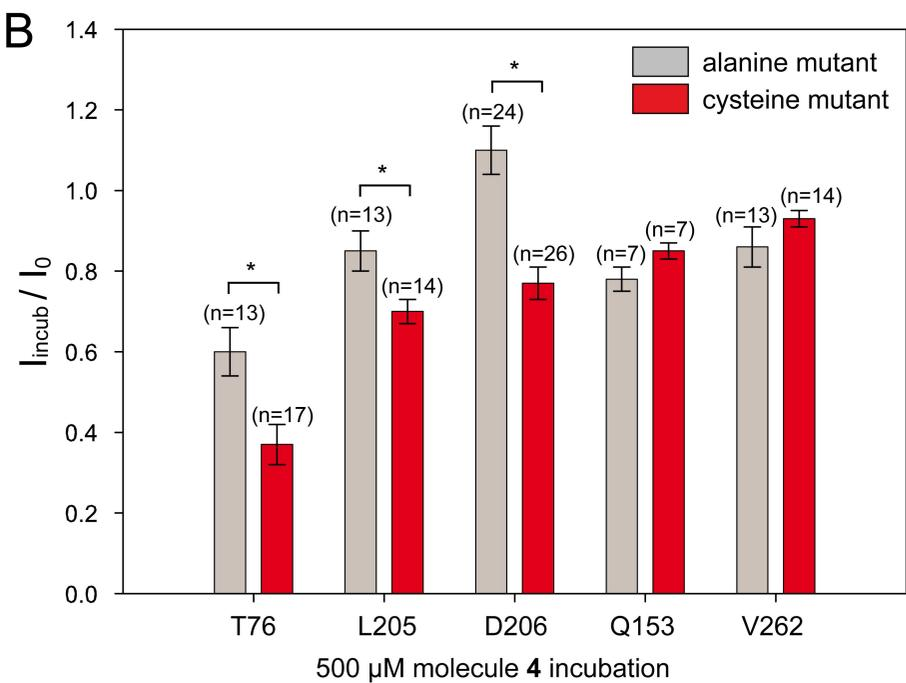
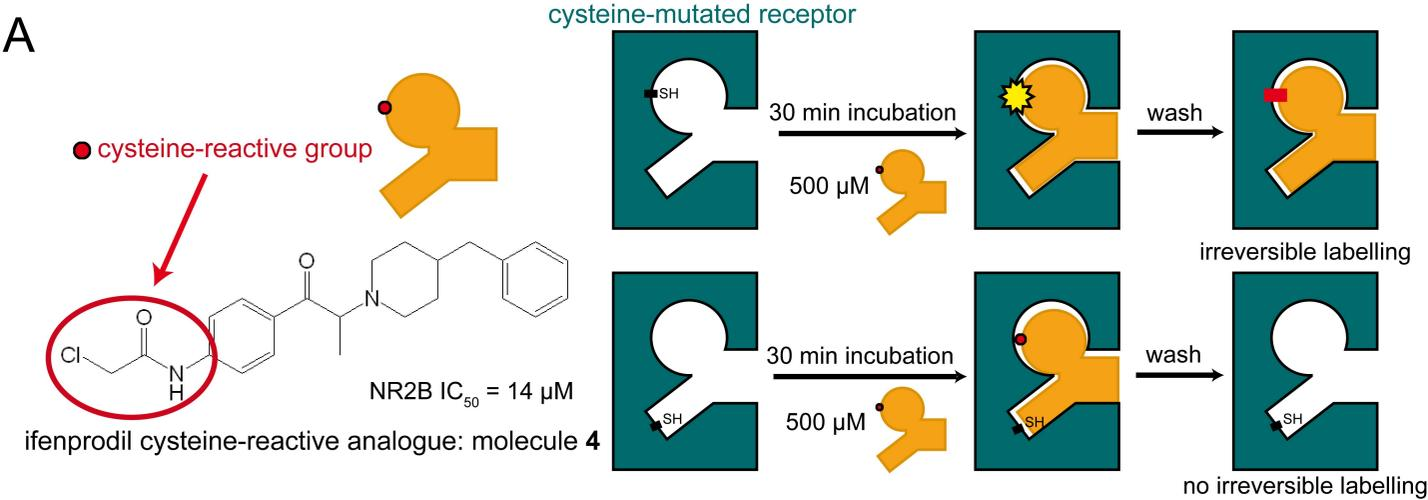


Figure 7